

MASSACHUSETTS INST OF TECH.  
DEPT OF CIVIL ENGINEERING  
RALPH M PARSONS LAB  
PORT NO. 90-5



# MODEL STUDY OF SEAWATER PURGING FOR THE BOSTON WASTEWATER OUTFALL

ENGINEERING LIBRARY  
TECHNICAL REPORT

by  
E. ERIC ADAMS  
DIRAK SAHOO  
and  
CHRISTOPHER R. LIRO

RALPH M. PARSONS LABORATORY  
HYDRODYNAMICS AND COASTAL ENGINEERING

Report Number 329

Prepared under the support of

Metcalf & Eddy, Inc.  
Woburn, Massachusetts

and the

Massachusetts Water Resources Authority  
Charlestown, Massachusetts

April, 1990

# MIT

DEPARTMENT  
OF  
CIVIL  
ENGINEERING

SCHOOL OF ENGINEERING  
MASSACHUSETTS INSTITUTE OF TECHNOLOGY  
Cambridge, Massachusetts 02139

# HYDRAULIC MODEL STUDY OF SEAWATER PURGING FOR THE BOSTON WASTEWATER OUTFALL

by  
E. ERIC ADAMS  
DIPAK SAHOO  
and  
CHRISTOPHER R. LIRO

**RALPH M. PARSONS LABORATORY**  
HYDRODYNAMICS AND COASTAL ENGINEERING

Report Number 329

Prepared under the support of  
Metcalf & Eddy, Inc.  
Woburn, Massachusetts  
and the  
Massachusetts Water Resources Authority  
Charlestown, Massachusetts

## Abstract

A 1:83 hydraulic scale model was built to study the mechanism of seawater purging in the tunneled outfall that will convey effluent from MWRA's Secondary Treatment Plant on Deer Is. out into Massachusetts Bay. Purging generally requires high rates of effluent flow which presents a concern for the Boston system because of the wide range of expected flow rates. Daily average flow rates are expected to range from about 320 mgd to 1270 mgd although instantaneous rates as low as 150 mgd may occur.

Model results for the original outfall design (described in the Secondary Treatment Facilities Plan) showed that riser purging would require an effluent flow rate of over 900 mgd, which is slightly less than the theoretical (Munro) criterion. Furthermore, because of the increase in tunnel invert slope beginning at the riser section, tunnel purging would require an effluent flow rate of over 800 mgd. Hence there would be significant periods of time when the effluent flow rate would be insufficient to purge seawater from either the tunnel or the riser sections of the outfall. The resulting unpurged condition would lead to poor distribution of the effluent within the receiving water and possible problems with sediment accumulation and biofouling within the tunnel. However, once purged the outfall would not experience seawater intrusion until flows dropped below the expected low-flow condition.

Construction of a tunnel constriction (Venturi section) just upstream from the risers was found to substantially reduce seawater penetration in the tunnel by creating a condition of densimetric critical flow. Theoretical calculations for a section with a 10' throat suggested that penetration could be eliminated for flows greater than about 420 mgd while observations showed elimination for flows greater than about 340 mgd. The lower observed flow is attributed to downstream mixing. The effluent flow rate required for riser purging would remain essentially the same—about 900 mgd.

Further tests showed that, in combination with the Venturi section, a short-term increase in effluent flow caused by intermittent dumping of the chlorine-contact tanks would significantly reduce the purging requirement. The release could be made through motorized gates and would require a peak flow of at least 700 mgd over a duration of 10 to 20 minutes. The total excess flow volume would be about 600,000 ft<sup>3</sup>, which is about one-third of the total volume and about one-half of the active volume of the chlorine-contact tanks. Because of the absence of seawater penetration upstream of the Venturi, this "rapid-purge" procedure would be successful at base flows down to 340 mgd or less, substantially increasing the periods of time when purging is possible.

## Acknowledgments

This study was sponsored by the Massachusetts Water Resources Authority, Boston, Mass., and by Metcalf and Eddy, Inc., Wakefield, Mass., under OSP 72065. The authors wish to thank Dr. Dominique Brocard of Metcalf and Eddy and Dr. Norman Brooks of Cal Tech (serving as consultant to Metcalf and Eddy) for their suggestions throughout the study. They also acknowledge the helpful assistance of Mitchell Stein, a summer intern student from Rutgers University.

## Table of Contents

	<u>page</u>
Abstract	2
Acknowledgments	3
Table of Contents	4
List of Figures	6
List of Tables	7
List of Symbols	8
1 Introduction	9
2 Background and Objective	9
2.1 Seawater Intrusion	13
2.2 Purging	14
2.2.1 Tunnel Purging	14
2.2.2 Riser Purging	16
2.2.3 Circulation Blocking	18
2.3 Model Objectives	18
3 Model Scaling	19
3.1 Length and Diameter Ratios	20
3.2 Flow Rate and Time Ratios	23
3.3 Chosen Model Ratios	24
4 Model Fabrication	27
4.1 Tunnel and Outfall	27
4.2 Risers and Ocean	27
5 Experiments and Observation	33
5.1 Verification of the Riser Headloss	33
5.2 Observations during Slowly Varying Flow Conditions	37
5.3 Transient Flow Tests; Sudden Release from the Chlorine-Contact Tanks	42
5.3.1 Observations of Tunnel Wedge Penetration	44
5.3.2 Observations of Purging	46
5.4 Variable Bathymetry	50
5.5 Riser Intrusion	54
5.6 Tests with Venturi Section	57

6 Summary and Conclusions	<u>page</u> 63
6.1 Basic Observations	64
6.2 Tests Simulating the Dumping of Chlorine-Contact Tanks	65
6.3 Sensitivity to Variable Bathymetry	66
6.4 Venturi	66
6.5 Salt Water Intrusion through Ports	68
7 References	68
Appendix Seawater Intrusion in a Partially Purged Diffuser	70

## List of Figures

	<u>page</u>
1 Map of Massachusetts Bay	10
2 Schematic diagram of the Boston tunnel outfall	11
3 Sketch of partially purged condition in diffuser	17
4 Moody diagram and friction factor (after Streeter and Wylie, 1979). In the prototype with old pipe ( $\epsilon/E = 4 \times 10^{-4}$ ), $f = 0.016$ for $Q$ between 320 mgd ( $Re = 2.4 \times 10^6$ ) to 1270 mgd ( $Re = 10^7$ ). For new pipe ( $\epsilon/D = 4 \times 10^{-5}$ ); $f \approx 0.011$ . In the model (smooth pipe) $f = 0.036$ ( $Re = 5.5 \times 10^3$ ) and $f = 0.025$ ( $Re = 2.2 \times 10^4$ ) for corresponding flowrates.	21
5 Diagram of model diffuser tunnel	28
6 Diagram of the riser offtake	29
7 Experimental set up of the riser and diffuser caps headloss measurement	31
8 Headloss in riser at various flows and port diameters	32
9 Schematic set up of the model	34
10 Hydraulic grade line along the section of tunnel modeled (prototype values). Outfall section is from 6600 ft to 132000 ft.	36
11 Hydrographs of various tests conducted. In test A flowrate is increased slowly. The slopes in B and C hydrographs are in gpm/sec (model).	38
12 Pressure distribution in purged (A) and unpurged (B) riser. $P_s$ is the hydrostatic pressure due to saltwater.	40
13 Wedge length vs. flowrate	45
14 Efficiency of purging vs. peak flow rates. $Q_{peak}$ is the flow at which the hydrograph is levelled off.	48
15 Riser elevation	51
16 Pressure distribution in non-uniform riser elevation	52
17 Pressure distribution during intrusion	56
18 Shape of Venturi	58
A1 Number of purged risers, $N-j$ , as a function of normalized effluent flow rate	71
A2 The pressure distribution in purged and unpurged risers with mixed flow	74
A3 Theoretical total downflow rate vs. effluent flow as a function of number of unpurged risers, $j$ . $Q_M$ is the Munro flow.	76
A4 Correlation of calculated downflow with experimental downflow	77
A5 Hysteresis in riser purging with increase and subsequent decrease in tunnel flow	80
A6 Rate of total energy loss at exit for varying number of purged risers	81

## List of Tables

	<u>page</u>
1 Nominal prototype values of diffuser design parameters	12
2 Prototype to model scaling ratios	25
3 Model values of diffuser parameters for $Q_0 = 650$ mgd and $\Delta r = \frac{1}{3}$	26
4 Purging flows in various tests	43
5 Excess water from chlorine-contact tanks required for purging	49
6 Excess water from chlorine-contact tanks required for purging with Venturi section	62
A1 Comparison of experimental and calculated total downflow	77



## List of Symbols

$b_f$	= ratio of upstream channel width to throat width in a lateral contraction
$c_f$	= friction factor (= $f/4$ )
$D$	= diameter of tunnel
$d$	= diameter of riser
$d_0$	= diameter of port
$F_c$	= densimetric Froude number at tunnel constriction
$F_0$	= densimetric Froude number of port discharge
$f$	= Darcy-Weisbach friction factor
$g$	= gravitational constant
$g'$	= $g\Delta$
$H$	= height of riser
$h_L$	= riser headloss
$j$	= number of unpurged risers or number of risers purging as a group
$L$	= length of the diffuser section
$L_{tun}$	= wedge length in tunnel
$N$	= number of risers
$n$	= number of ports per riser
$Q, Q_0$	= flow rate in tunnel
$Q_b$	= base flow in tunnel
$Q_I$	= minimum flow to prevent riser intrusion
$Q_M$	= Munro flow; theoretical flow rate required for riser purging
$Q_{ris}$	= flow for riser purging
$Q_{tun}$	= flow for tunnel purging
$q_i$	= flow rate in riser
$R$	= Reynolds number
$Ri$	= bulk Richardson number
$t$	= time
$U$	= velocity in diffuser tunnel
$U_*$	= friction velocity
$u_0$	= velocity in port
$V_e$	= entrainment velocity
$\alpha$	= a system parameter governing riser headloss
$\Delta$	= $\frac{\rho_s - \rho}{\rho}$
$\epsilon$	= pipe roughness height
$\theta$	= slope of tunnel
$\rho$	= density of effluent
$\rho_s$	= density of seawater
$\nu$	= kinematic viscosity of water

subscript c = value at throat of lateral constriction  
 subscript m = value of parameter in model  
 subscript p = value of parameter in prototype  
 subscript r = ratio of prototype value to model value

## 1 INTRODUCTION

This report describes physical model studies concerning the Boston Wastewater Outfall Tunnel. The studies examine the mechanism of purging of seawater from the tunnel and risers.

The tunnel will discharge treated effluent into Massachusetts Bay (Figure 1) at daily average flow rates ranging from 320 to 1270 mgd. Instantaneously, however, flowrates as low as 150 mgd may be expected. According to preliminary design information (Secondary Treatment Facilities Plan, Vol. 5, MWRA (1988)), the tunnel will be about 24.3 ft in diameter and 50,000 ft in length with a 1:2000 upward slope, and will end in a 6600-ft diffuser section with about 80 risers (Figure 2).<sup>1</sup> The riser section will be tapered with decreasing cross section area to allow near-constant tunnel velocities. The decreasing cross section will be obtained by increasing the slope of the tunnel invert while leaving the soffit slope essentially unchanged. Each riser will have a diffuser cap at the top with eight ports per cap. The ports are designed to discharge flow horizontally with a radial distribution. The risers will be connected to the bottom of the tunnel and rise about 250 ft to the sea floor. Table 1 gives the nominal prototype values of the diffuser design parameters.

## 2 BACKGROUND AND OBJECTIVE

Ocean outfalls that extend several miles offshore and include a multi-port diffuser are an economical means of effluent disposal. Such outfalls may be constructed either by tunnelling, or by laying a pipeline in a trench cut in the seabed. The

---

<sup>1</sup>It should be added that, during this study, the number of risers was changed from 80 to 55, based on dilution modeling (Roberts, 1989); this change is not expected to affect the purging process.

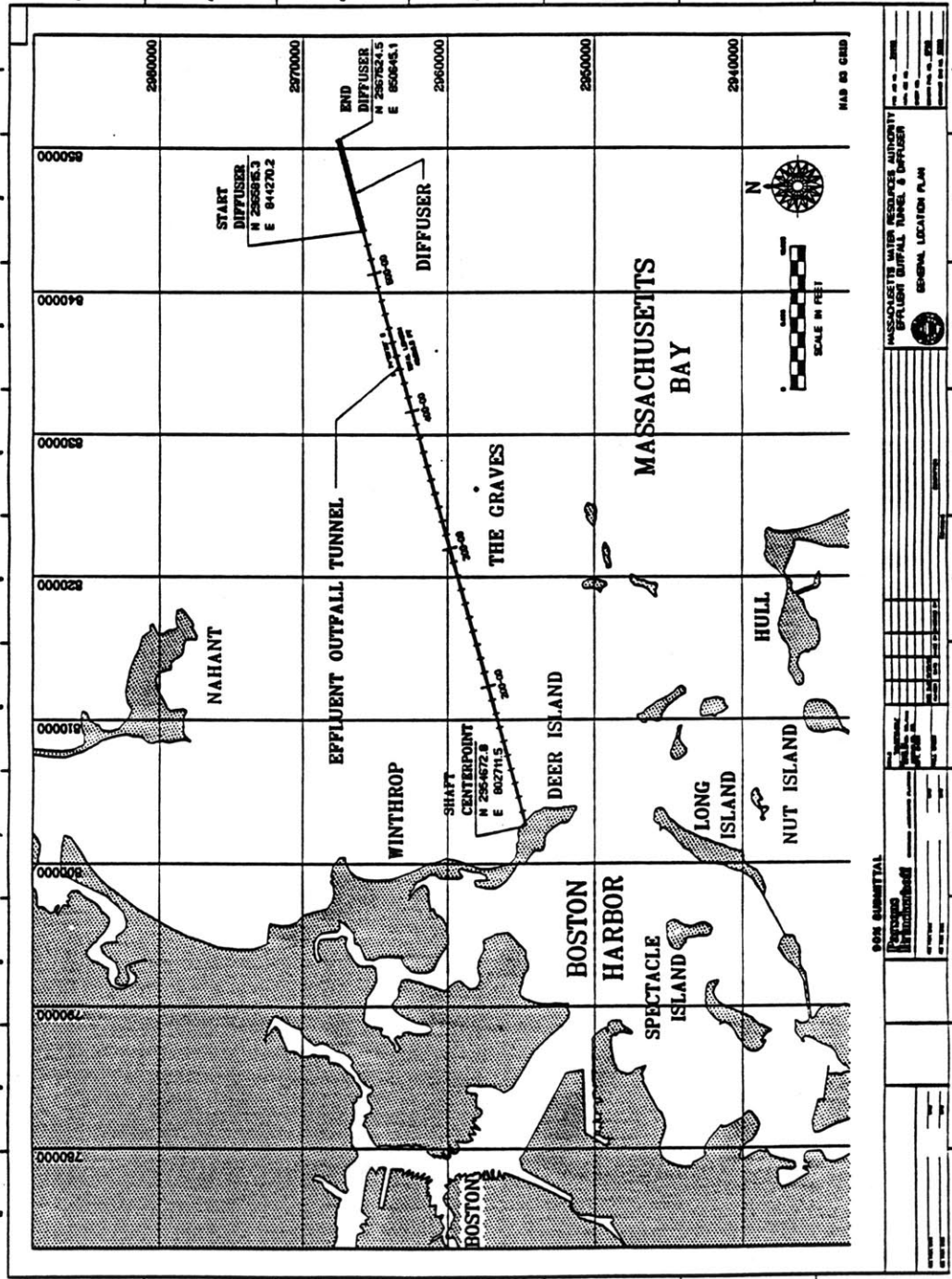
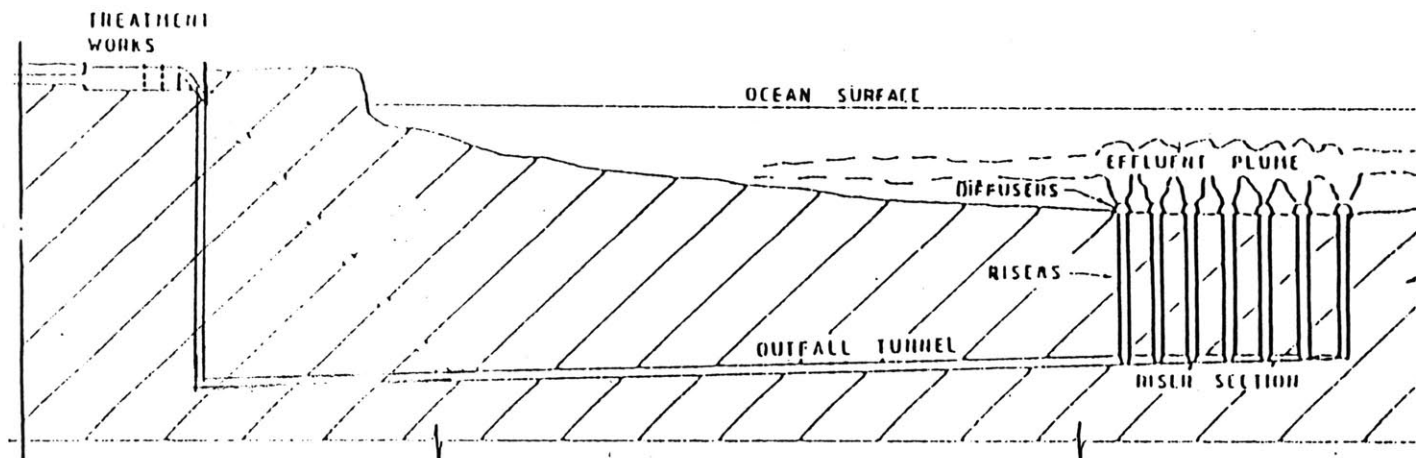


Figure 1 Map of Massachusetts Bay



**Model dimensions:**  
 tunnel diameter = 3.5 in  
 riser height = 35.6 in  
 diffuser section = 40 ft  
 number of risers = 80  
 flow rate = 6.2 to 25 gpm

**Prototype dimensions:**  
 tunnel length = 50,000 ft (9 miles)  
 tunnel diameter = 24 ft  
 tunnel depth (from seabed) = 235 ft  
 number of risers = 80; later changed to 55  
 diffuser section = 6600 ft  
 flow rate = 500 to 2000 cfs

Figure 2 Schematic diagram of the Boston tunnel outfall

Table 1  
Nominal Prototype Values of Diffuser Design Parameters

<u>Parameter</u>	<u>Symbol</u>	<u>Value</u>
diameter of tunnel	D	24.3 ft
diffuser length	L	6600 ft
riser height	H	247 ft
tunnel slope	$\sin \theta$	1/2000 upward
number of risers	N	80
number of ports/riser	n	8
riser diameter	d	2.5 ft
port diameter	$d_0$	0.42 ft
effluent flow rate	Q	320-1270 gpm (500 - 1970 cfs)
port discharge velocity	$u_0$	5.6 - 22.6 ft/s
relative density diff	$\Delta = \frac{\rho_s - \rho}{\rho}$	0.027
tunnel rel. roughness (new)	$\epsilon/D$	$4 \times 10^{-5}$
tunnel rel. roughness (old)	$\epsilon/D$	$4 \times 10^{-4}$
tunnel friction factor (new)	f	0.011
tunnel friction factor (old)	f	0.016

former option, which has been chosen for the Boston outfall, allows protection from waves and reduces environmental disruption during construction. There are presently fewer than ten tunneled outfalls throughout the world, with several under construction or in design stage, including three in Sydney, Australia.

Several existing tunneled outfalls have not performed up to design expectations due to the fact that effluent discharges only from some of the risers. This condition is accompanied by seawater intrusion into the remaining risers and results from incomplete purging of seawater residing in the tunnel prior to start-up. The presence of seawater in an outfall results in hydraulic inefficiencies, causing decreased dilution with ambient receiving water and increased head loss. More importantly, seawater circulation can cause marine biofouling and collection of sediments in the tunnel resulting in partial failure of some tunnels (Bennet 1981, Charlton 1982). The mechanisms of purging, along with several related processes, are discussed briefly below.

## 2.1 Seawater Intrusion

Seawater may intrude through the diffuser ports if the port is not flowing full with effluent. It is recommended that the densimetric Froude number of the port discharge ( $F_0$ ) be above unity to prevent intrusion (Brooks 1970).

$$F_0 = \frac{u_0}{\sqrt{\frac{\Delta\rho}{\rho}gd_0}} > 1 \quad (1)$$

Allowing a factor of 2 for safety, a criterion for the effluent flow  $Q_I$  required to prevent riser intrusion is

$$Q_I = 2nN\frac{\pi}{4} d_0^3 \sqrt{\frac{\Delta\rho}{\rho}gd_0} \quad (2)$$

where  $u_0$  is the port velocity,  $d_0$  is the port diameter,  $N$  is the number of risers,  $n$  is the number of ports per riser, and  $\Delta\rho/\rho$  is the normalized difference between seawater density  $\rho_s$  and effluent density  $\rho$ .

Experiments by Wilkinson (1988a) conducted at near-prototype scales and with varying port shape and intrusion confirmed Brooks's basic criterion. In no case was intrusion observed for  $F_0 > 1$ . The experiments showed that orifice ports were somewhat more resistant to intrusion than were nozzle ports and that about twice the flow was required to prevent intrusion in ports discharging horizontally than in ports discharging vertically; i.e., the critical value of  $F_0$  for a horizontal port orientation was about 0.7, while that for vertical jets was about 0.3 - 0.4 depending on port shape. The experiments were conducted for a single port diffuser, but since interference from adjacent ports is unlikely, the results should be applicable for cases with more than one port. However one must first compute the riser flow distribution in order to relate an intrusion criterion based on flow per riser to one based on total diffuser flow.

## 2.2 Purging

It is desirable that the outfall be purged of any seawater both in the diffuser tunnel and in the individual risers. Somewhat different criteria—as well as potential remedies—apply to these two cases.

2.2.1 Tunnel Purging. Purging of seawater from the diffuser tunnel requires that the tunnel “flow full” of effluent which should occur if the flow rate is large enough

and the tunnel slope is small enough. Under conditions of uniform pipe diameter, Wilkinson (1988b) gives this criterion as

$$Q_{\text{tun}} > \left[ \frac{2D \Delta\rho/\rho g \sin\theta}{f} \right]^{\frac{1}{2}} \frac{\pi D^2}{4} \quad (3)$$

where  $Q_{\text{tun}}$  is the effluent flow,  $\theta$  is the tunnel slope, and  $D$  is the tunnel diameter. This criterion is similar to that governing the inverted situation of having full pipe flow where air is the fluid being expelled by water.

Eq. (3) assumes uniform flow and, even if this criterion is satisfied, a saltwater wedge may still persist upstream from the diffuser section (gradually varied flow). The extent of wedge penetration depends on downstream boundary conditions (i.e., depth of saltwater at the beginning of the riser section). For example, if the slope of the tunnel invert increases beginning at the riser section, as is the case with the Boston outfall, then the steeper slope will make it more difficult to purge saltwater from the riser section of the tunnel than the upstream tunnel section. The ability to purge the riser section will thus govern upstream saltwater penetration.

A different condition occurs if there is a sudden expansion in the tunnel (e.g., if a constriction is placed upstream of the riser section), in which case seawater penetration will be governed by a condition of densimetric critical flow, controlled by a densimetric Froude number. Armi and Farmer (1986) studied flow in vertical-wall channels with lateral contractions characterized by varying ratios  $b_f$  of upstream channel width to throat width. They found that wedge penetration was eliminated if flow exceeded a critical value of  $F_c$  ranging from 0.54 ( $b_f \rightarrow \infty$ ) to 0.58 ( $b_f = 2.0$ ) to 1.0 ( $b_f \rightarrow 1.0$ ).  $F_c$  is defined by

$$F_c = \frac{Q}{\sqrt{g(\Delta\rho/\rho)H^3B^2}} \quad (4)$$



where H and B are the tunnel depth and width at the constriction. In either of these two cases, the extent of upstream wedge penetration can be found theoretically by a backwater calculation based on downstream interfacial conditions between effluent and seawater.

2.2.2 Riser Purging. Figure 3 shows a schematic representation of a partially purged diffuser. Purging of an individual riser requires that, at the riser offtake, the tunnel pressure exceed the hydrostatic pressure associated with the weight of seawater above the offtake. Using the elevation of the riser cap as a datum, the tunnel pressure head consists of a hydrostatic term (associated with the effluent density) and an internal head loss due to downstream losses in the tunnel and risers. Hence riser purging requires that the internal head loss ( $h_L$ ) exceed the *differential* hydrostatic pressure head based on the riser height and the difference in density between seawater and effluent or  $\Delta\rho H/\rho$  where H is the riser height. The latter head is referred to as the Munro head and this basic criterion is known as the Munro Criterion.

$h_L$  will comprise mainly the exit head loss at the riser discharge port and will be proportional to the square of the discharge flow in each riser,  $q_i$ , i.e.,

$$h_L = \alpha q_i^2 \quad (5)$$

If we assume equal flow through all risers, that riser heights are all equal, that there is no downward flow through unpurged risers, and that the number of risers N is large, the Munro criterion becomes

$$Q_M = N \sqrt{\frac{\Delta\rho H}{\alpha\rho}} \quad (6)$$

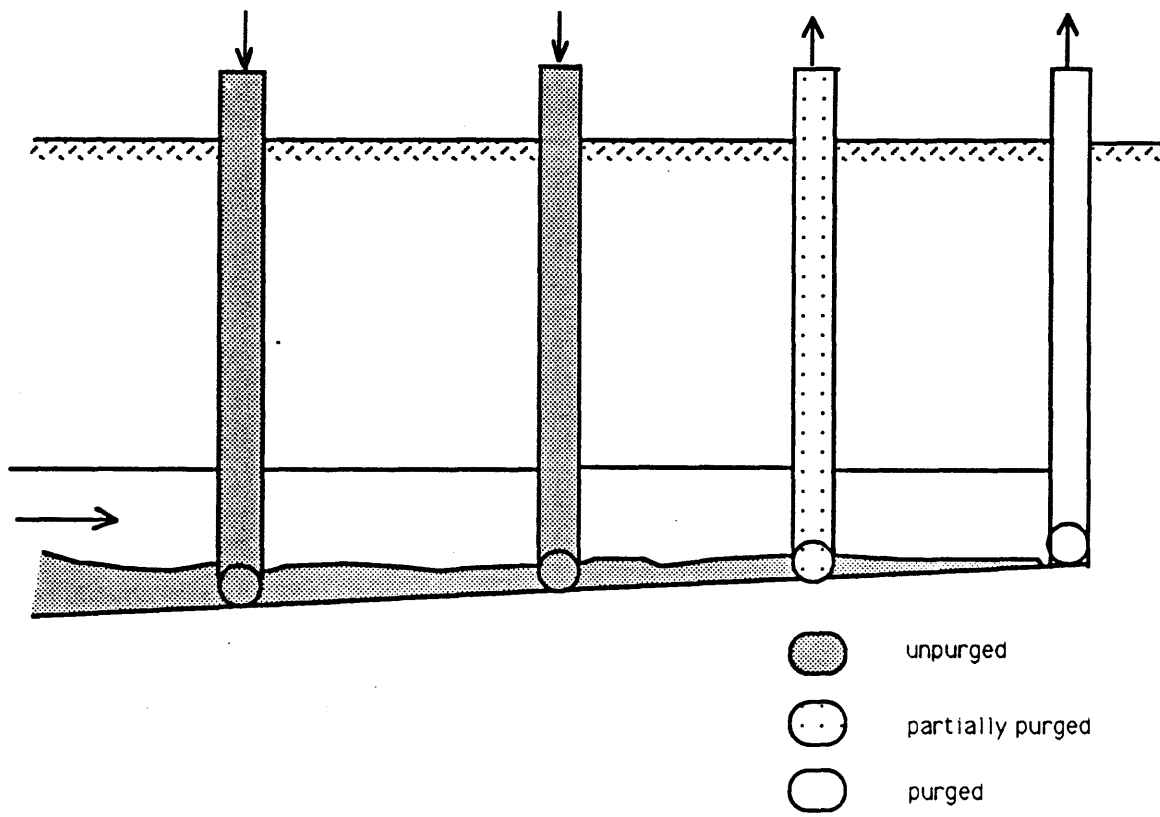


Figure 3 Sketch of partially purged condition in diffuser

$Q_M$  is the Munro flow and  $\alpha$  is a proportionality constant with dimensions of  $\text{time}^2/\text{length}^5$ . Modifications to Eq. (6) accounting for downward flow in unpurged risers are discussed in the appendix.

2.2.3 Circulation Blocking. A related phenomenon is called circulation blocking (Charlton 1982). There are several mechanisms by which circulation blocking may occur.

When effluent flow is stopped, the forward momentum of the effluent in the tunnel carries it toward the seaward risers. This causes the denser seawater to enter the shoreward risers and a quasi-steady-state gravitational circulation may persist for hours. If the effluent flow is restarted during this period the circulation is reinforced and may persist longer.

Circulation blocking can also occur due to passage of long gravity waves on the surface. The spatial variation in pressure results in effluent outflow in some risers and seawater intrusion in others. Brooks (1988) suggested that such circulation could also occur if the tunnel slopes strongly (upward) in the offshore direction. The higher-elevation seaward risers would purge first and, due to the higher column of dense seawater in the shoreward risers, the excess pressure would allow seawater to intrude through the shoreward risers. Circulation blocking has been analyzed by Wilkinson (1985), who gives a criterion for prevention that is similar to the Munro criterion.

### 2.3 Model Objectives

In view of the above discussion, our study has the following objectives with regard to the MWRA Wastewater Outfall:

1) To analyze the mechanisms of riser and tunnel purging, seawater penetration into and entrainment from the tunnel, and seawater intrusion into the risers.

2) To determine the validity of Munro's criterion under both steady and time-varying flows

3) To estimate the time scale of the processes

4) To examine measures needed to prevent wedge penetration and achieve purging

### 3 MODEL SCALING

Hydraulic modeling requires geometric, kinematic, and dynamic similitude. To achieve dynamic similitude the following dimensionless group should, ideally, be the same in the model and the prototype.

$$\text{Densimetric Froude Number } \mathbb{F} = \frac{U}{\sqrt{g(\Delta\rho/\rho)D}}$$

$$\text{Reynolds Number } \mathbb{R} = \frac{UD}{\nu}$$

$$\text{Friction Factor } f$$

where  $\nu$  is the kinematic viscosity.

In practice one can not have all the dimensionless numbers the same in the model and the prototype. Because of the interplay of inertial and buoyancy forces, the densimetric Froude number,  $\mathbb{F}$ , is of paramount importance and should be equal in model and prototype. Using a subscript r to describe the ratio of a prototype quantity (subscript p) to a model quantity (subscript m),

$$F_r = 1 \quad (7a)$$

To simulate the purging process in the risers Eq. (7a) translates to

$$F_r = \frac{U_r^2}{\Delta_r D_r} = 1 \quad (7b)$$

where  $\Delta = \Delta\rho/\rho$ .

### 3.1 Length and Diameter Ratios

Lengths are generally smaller in a model than in prototype, so the Reynolds number ratio  $R_r$  is usually larger than one. The major implication of  $R_r \neq 1$  is the effect on friction factor and the ratio  $f_r$ . Using Eq. (7), the model and prototype Reynolds numbers are related by

$$R_r = U_r D_r = \Delta_r^{1/2} D_r^{3/2} \quad (8)$$

Referring to a Moody diagram (Figure 4), because  $R_m$  is less than  $R_p$ ,  $f_m$  is generally larger than  $f_p$ , even when the model pipe is smooth.

Since head losses depend on friction factor, the only recourse in this case is to use a distorted model. Following Wilkinson (1988b) the slope ratio is given by

$$(\sin \theta)_r = f_r \quad (9)$$

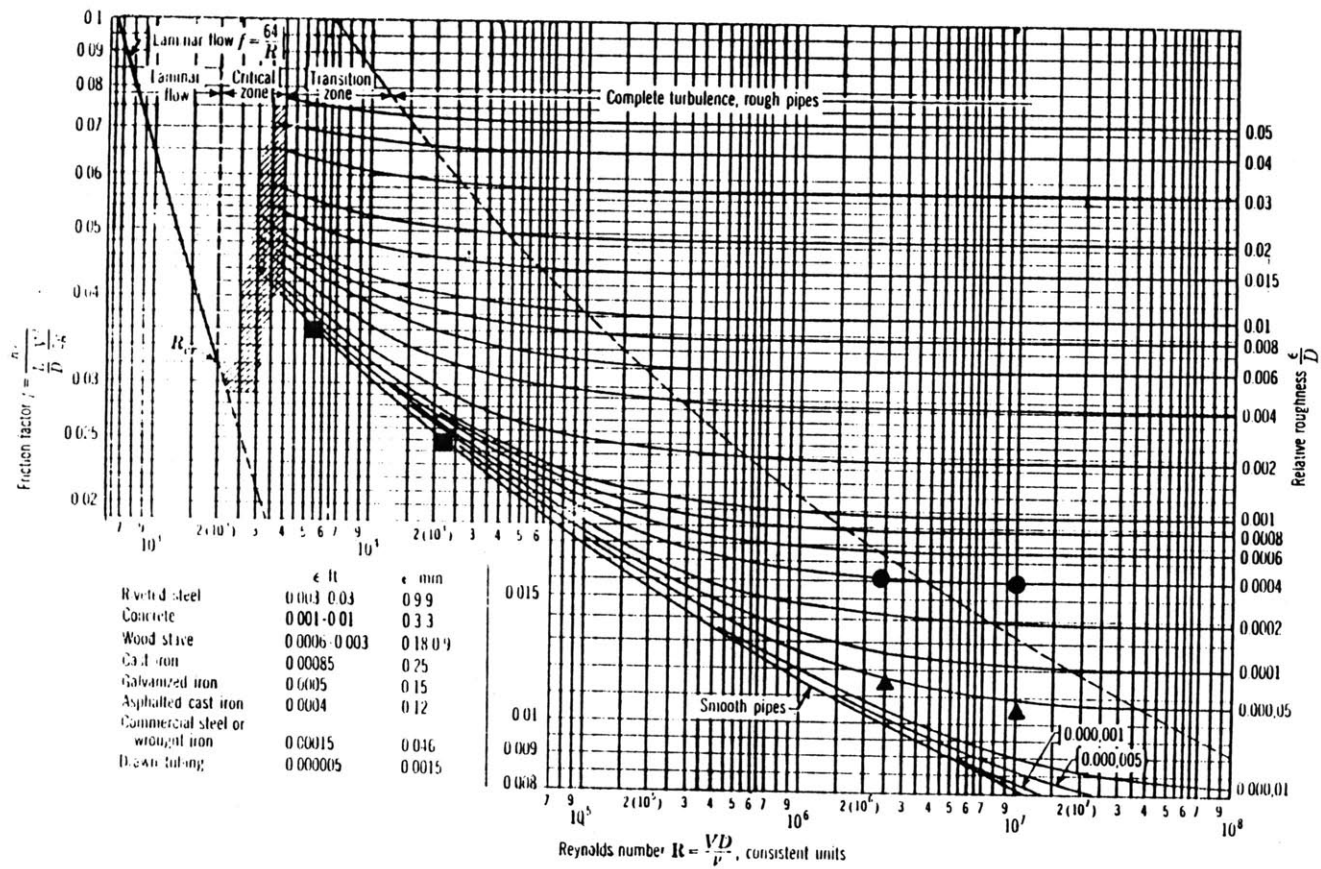


Figure 4 Moody diagram and friction factor (after Streeter and Wylie, 1979). In the prototype with old pipe ( $\epsilon/E = 4 \times 10^{-4}$ ; ●),  $f = 0.016$  for  $Q$  between 320 mgd ( $Re = 2.4 \times 10^6$ ) to 1270 mgd ( $Re = 10^7$ ). For new pipe ( $\epsilon/D = 4 \times 10^{-5}$ ; ▲);  $f \approx 0.011$ . In the model (smooth pipe; ■)  $f = 0.036$  ( $Re = 5.5 \times 10^3$ ) and  $f = 0.025$  ( $Re = 2.2 \times 10^4$ ) for corresponding flowrates.

Eq. (9) states that the model slope must be increased in proportion to the increase in friction in order for the gravity force to balance friction. Hence the vertical (and diameter) scales must be exaggerated compared to the horizontal as given by

$$\frac{L_r}{D_r} = f_r^{-1} \quad (10)$$

The distortion ratio given by Eq. (10) is based on the objective of properly scaling the hydraulic grade line. An alternative distortion ratio has been suggested by Wilkinson (1988b) based on the objective of correctly scaling the ratio of entrained flow (from the arrested saltwater wedge in the tunnel) to the effluent flow rate itself. This criterion may be important because removal of a wedge from the tunnel is governed by entrainment when the flow is less than the tunnel purging flow. The entrainment is a function of the bulk Richardson number,  $Ri_*$  (Turner, 1973),

$$Ri_* = \frac{g \frac{\Delta \rho}{\rho} D}{U_*^2} \quad (11)$$

Wilkinson (1988b) uses

$$\frac{V_e}{U_*} = k Ri_*^{-3/2} \quad (\text{for } Ri_* > 10) \quad (12)$$

where  $V_e$  is the velocity of entrainment,  $U_*$  is the friction velocity given by

$$U_*^2 = C_f U^2 \quad (13)$$

and  $k$  is a constant. The total entrainment rate  $Q_e$  scales as the product of  $V_e$  times the wedge length times the tunnel diameter. Substituting  $f_r$  for  $C_{fr}$ , this yields

$$\left[\frac{Q_e}{Q}\right]_r = f_r^2 \left[\frac{L_r}{D_r}\right] \quad (14)$$

Requiring  $(Q_e/Q)_r = 1$  thus requires that the distortion ration  $L_r/D_r$  be given by

$$\frac{L_r}{D_r} = f_r^{-2} \quad (15)$$

or somewhat greater than that given by Eq. (10).

Because our model does not include the entire tunnel length, it is not possible to simulate the entrainment process under conditions where the saltwater wedge extends upstream beyond the model boundaries. Hence model distortion was based on Eq. (10). Note that use of Eq. (10) rather than (15) is somewhat non-conservative in the sense that it overestimates entrainment.

### 3.2 Flow Rate and Time Ratios

The flow rate is governed by

$$Q_r = U_r D_r^2 = \Delta_r^{1/2} D_r^{5/2} \quad (16)$$

Due to the geometric distortion, tunnel purging and riser purging have different time scales. A time scale, in general, is obtained by dividing a volume by a flow rate. For tunnel purging



$$t_r = \frac{L_r D_r^2}{Q_r} = \frac{L_r}{\Delta_r^{\frac{1}{2}} D_r^{\frac{1}{2}}} \quad (17)$$

while for riser purging

$$t_r = \frac{H_r D_r^2}{Q_r} = \frac{D_r^3}{Q_r} = \frac{D_r^{\frac{3}{2}}}{\Delta_r^{\frac{1}{2}}} \quad (18)$$

where  $H_r (= D_r)$  is the height ratio.

### 3.3 Chosen Model Ratios

Due to the availability of plastic pipe and size limitations, a diameter ratio of  $D_r = 83$  was chosen (corresponding to nominal 4" plexiglas pipe with 3.5" ID). In order to maximize  $R_m$ , density differences (salinities) were increased in the model (i.e.,  $\Delta_r < 1$ ), and a nominal value of  $\Delta_r = \frac{1}{3}$  was used. For the chosen  $D_r$  and  $\Delta_r$ ,  $R_r$  may be computed from Eq. (8) and  $f_r$  can be obtained from a Moody diagram as a function of prototype flow rate.

The model  $R_m = 1.1 \times 10^4$ , corresponding to a prototype flow of about 650 mgd (1000 cfs), gives a model friction factor  $f$  (smooth pipe) of 0.03. The prototype tunnel (new pipe) will have a relative roughness of about  $4 \times 10^{-5}$  and at 650 mgd this corresponds to  $f = 0.011$ . (See Figure 4.) For old pipe the relative roughness will be about  $4 \times 10^{-4}$  corresponding to  $f = 0.016$ . Thus for old pipe and this flow rate  $f_r \approx 0.5$ . A value of  $f_r = 0.5$  has been used to determine the model slope and distortion ratios by Eqs. (9) and (10) respectively. Scaling ratios applicable for the diffuser parameters are listed in Table 2. Model parameters corresponding to prototype values in Table 1, are listed in Table 3.

Table 2  
 Prototype to Model Scaling Ratios

	<u>relation</u>	magnitude at $Q = 650 \text{ mgd}$ and $\Delta_r = 1/3$
diameter	$D_r$	83
density difference	$\Delta_r$	0.33
friction factor	$f_r$	0.5
length	$L_r = D_r f_r^{-1}$	166
velocity	$U_r = [\Delta_r D_r]^{1/2}$	5.2
flow rate	$Q_r = [\Delta_r D_r^5]^{1/2}$	$3.6 \times 10^4$
Reynolds number	$R_r = [\Delta_r D_r^3]^{1/2}$	440
Time scales:		
tunnel purging	$t_r = \frac{L_r}{\Delta_r^{1/2} D_r^{1/2}}$	32
riser purging	$t_r = \frac{D_r^{1/2}}{\Delta_r^{1/2}}$	16
slope ratio	$(\sin \theta)_r = f_r$	0.5

Table 3  
 Model Values of Diffuser Parameters for  $Q = 650$  mgd and  $\Delta_r = \frac{1}{4}$

<u>Model parameter</u>	<u>Symbol</u>	<u>Value</u>
diameter of tunnel	D	3.5 in
velocity	U	0.42 ft/s
flow rate	Q	12.5 gpm
Tunnel Reynolds number	R	$1.1 \times 10^4$
friction factor	f	.03
slope	( $\sin \theta$ )	$10^{-3}$
length of diffuser (outfall section)	L	40
height of riser	H	3 ft
diameter of riser	d	0.37 in

## 4 MODEL FABRICATION

### 4.1 Tunnel and Outfall

The tunnel was modeled using 4 in nominal (3.5 in ID) pipe. Since most of the observations were visual, the pipe was made of clear plexiglas. The 40' (6600' prototype) diffuser section and another 40' of tunnel immediately upstream of the diffuser were simulated. The model was fabricated using discrete lengths (4 feet) of pipe connected by flanges so that it could be extended if necessary.

To achieve constant velocities within the riser section each circular pipe section was cut and replaced by a flat "floor" whose elevation rises with distance downstream to decrease the flow area. At about the mid point of the diffuser section (19.5 feet downstream) a transition was made to nominal 3 in plexiglas (2.5 in ID). The last 5 feet of the riser section had a uniform diffuser cross section because a progressively smaller cross section area would create both flow and construction difficulties. Figure 5 shows a typical longitudinal cross section view of the diffuser pipe.

### 4.2 Risers and Ocean

The risers were constructed out of  $\frac{1}{4}$  in (nominal) and 0.37 in (ID) Lexan tubes. The risers were spaced 6 in apart and rose to a height of about 3 feet from the bottom of the diffuser tunnel.

The offtake of each riser was horizontal, flush with the bottom of the tunnel and oriented at a 45° angle to the tunnel<sup>2</sup>. The risers curve up smoothly with a radius

---

<sup>2</sup>In the final design this angle was changed to 90°, but the change is not expected to affect the validity of the model.

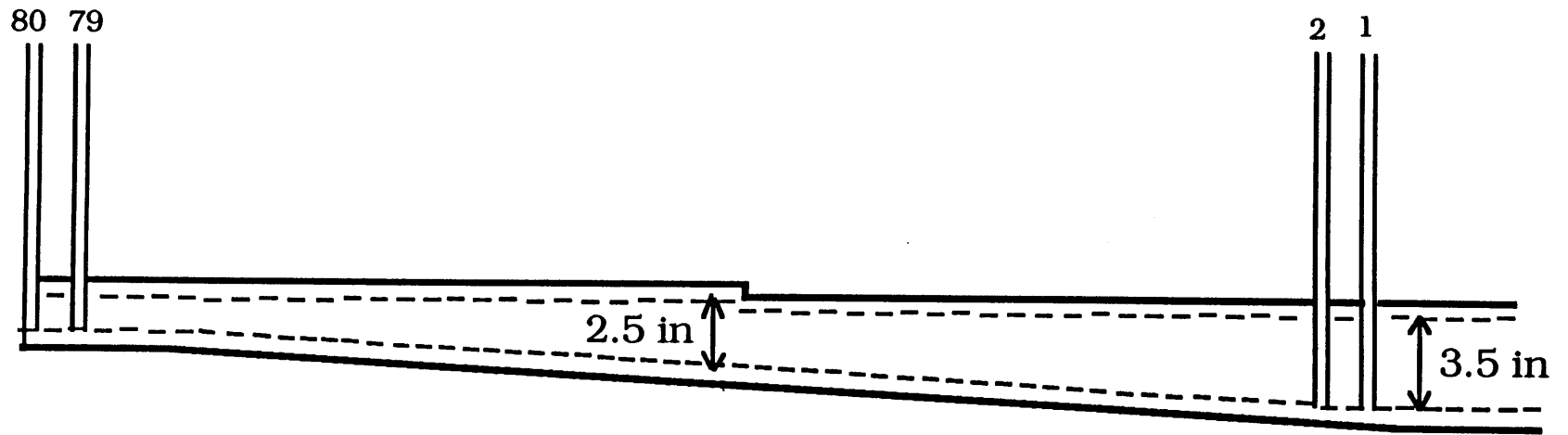


Figure 5 Diagram of model diffuser tunnel

of curvature approximately equal to the radius of the tunnel (see Figure 6). For initial tests, all diffuser caps were at the same elevation. The caps consisted of plugged PVC tees, each with two ports of diameter 0.136 in drilled through them.

It can be noted that the two-port tee riser caps used in the model are somewhat different in shape from the eight-port riser caps anticipated for the prototype. This is not a concern because the main objective of the model risers and caps was merely to simulate equivalent headloss, since headloss governs application of the Munro purging criterion (see Eq. (5), (6)). The prototype outfall is to be designed to purge at approximately 80% of peak flow which translates to about 1030 mgd or 19.8 gpm in the model. Because of its easy availability a PVC tee connection with plugs was chosen to represent a two-port diffuser. Holes of different size were drilled into a number of sample plugs in order to identify the hole size that came closest to the correct headloss at 19.8 gpm. The headloss design experiments were carried out with a single riser using freshwater, and the results (i.e., optimal port size) were applied to all the risers, which presumes a uniform flow in all purged risers. The riser height in the headloss model was 35.4" so for a prototype-to-model density difference ratio of 1/3, the required headloss is

$$h_{Lm} = \left[ \frac{\Delta\rho H}{\rho} \right]_m = .027 \times 3 \times 35.4 = 2.9 \text{ in}$$

The schematic of the experimental set up is given in Figure 7. The resulting headloss for various port diameters and flows are shown in Figure 8. By trial and error a port diameter of  $d_0 = 0.136$  in was chosen.

It might be added that, while the model riser caps were designed solely to reproduce headloss, the chosen diameter of 0.136 in scales fairly closely to the prototype value. The 80-riser design with eight ports per riser has port diameter of

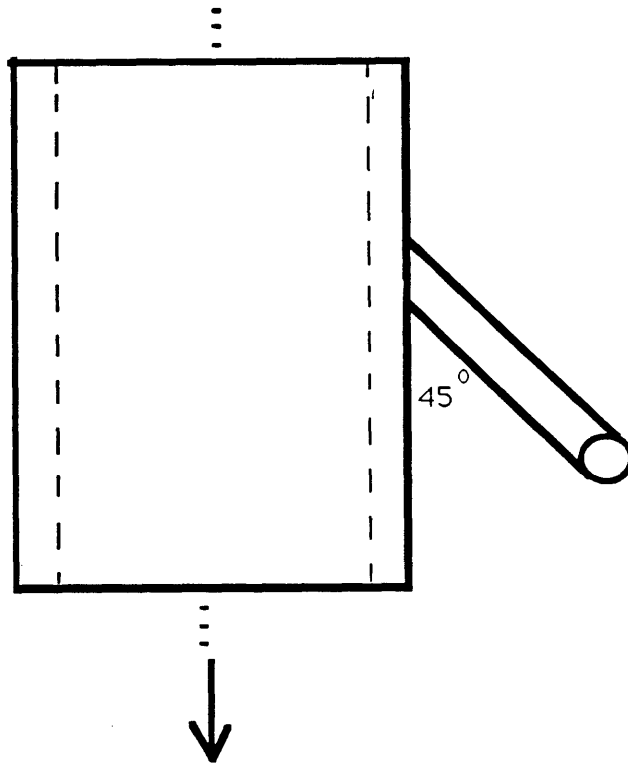
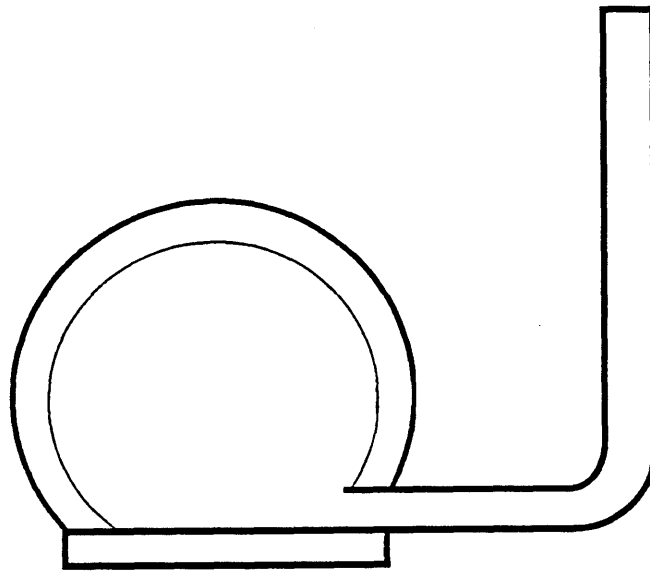


Figure 6 Diagram of the riser offtake

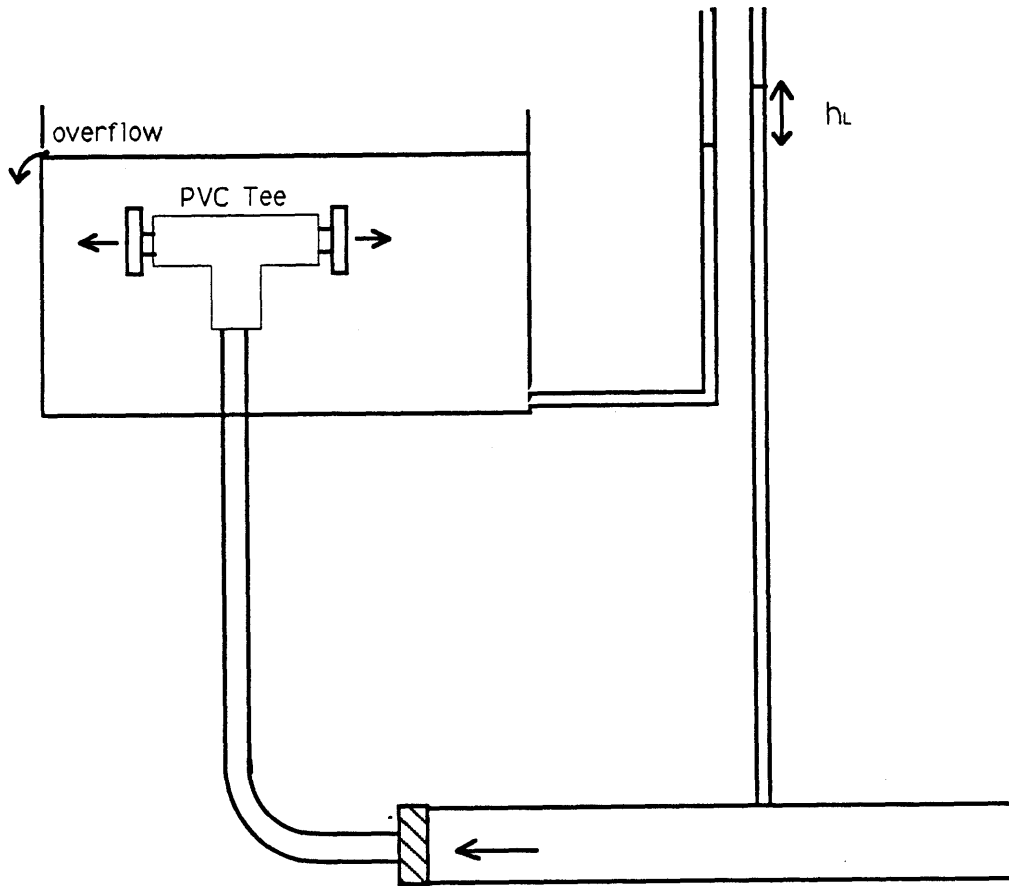


Figure 7 Experimental set up of the riser and diffuser caps headloss measurement



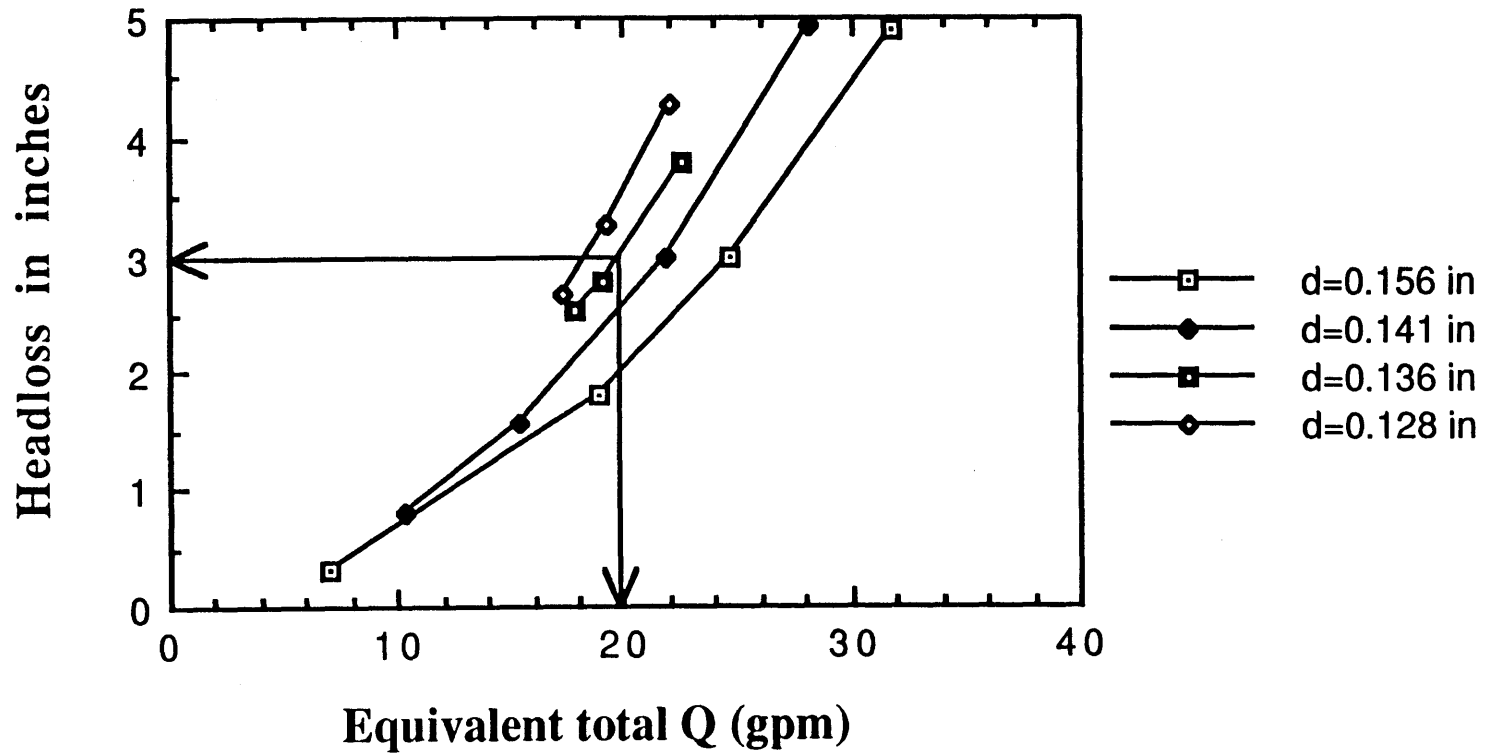


Figure 8 Headloss in riser at various flows and port diameters

0.42 ft (prototype; see Table 1). The equivalent diameter in a two-port riser (giving equal exit velocity) would be 0.84 ft and dividing by  $D_r = 83$  gives a diameter of 0.121 in or about 11% less than 0.136 in. The difference is likely due, in part, to a lower nozzle discharge coefficient in the model.

The risers entered the overhead tank from below. The overhead tank served as the ocean and was constructed with marine plywood of dimensions 32"W × 16"H × 40'L. It held dyed salt water and one side was made of plexiglas for ease of visualization. An adjustable drain at the surface allowed salt water to overflow when the model was operated. Figure 9 shows the overall experimental design including the circulating pump used to generate uniform salinity prior to the start of any experiment.

## 5 EXPERIMENTS AND OBSERVATION

A number of experiments were conducted with the model to achieve the objectives outlined earlier. The observations of riser and tunnel purging were made visually, by using clear freshwater (effluent) and dyed (blue FD&C #1) salt water. Observations of seawater intrusion through individual risers were also made by injecting Rhodamine WT (red) dye into the receiving water near the riser ports. Measurements of seawater and effluent density were made with a calibrated stem hydrometer (precision = 0.0005 g/cm<sup>3</sup>) by withdrawing samples from different depths and locations in the tank (to measure seawater) and from the tunnel (to measure effluent).

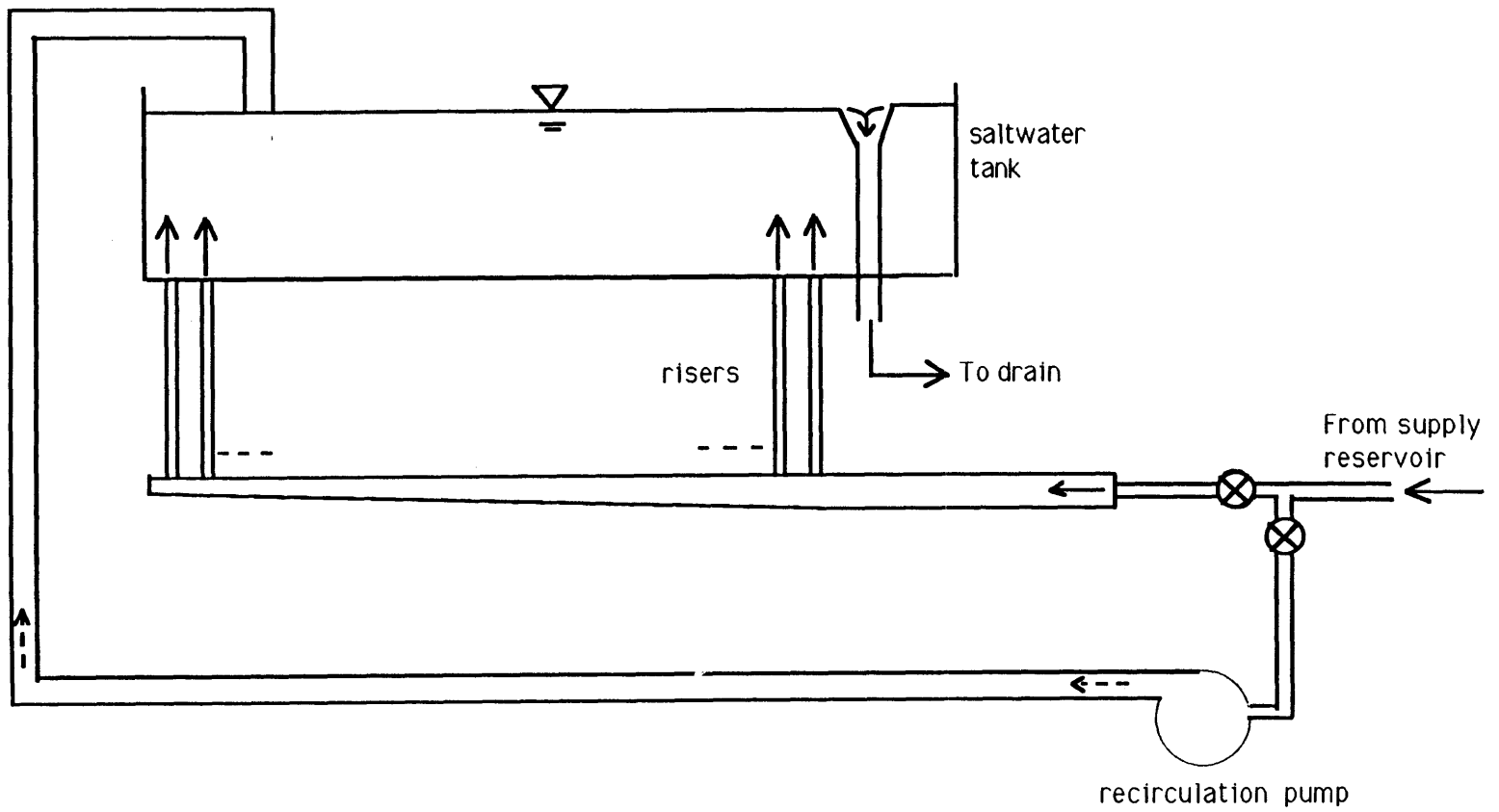


Figure 9 Schematic set up of the model

## 5.1 Verification of the Riser Headloss

Once all risers were constructed, the system was run with only freshwater to establish the hydraulic grade line. Manometers were installed at the upstream end of the tunnel ( $x = 0$  in Figure 10) and at 4-foot intervals along the riser section ( $40 < x < 80$  ft in the model;  $6600 < x < 13200$  ft in the prototype). As discussed in the previous section, the tunnel was designed to achieve riser purging at a model flow of 19.8 gpm (1030 mgd, or approximately 80% of the design maximum flow).

Figure 10 plots the observed head loss ( $h_L$ ) at  $Q_M = 19.8$  gpm (1030 mgd) and the Munro head ( $\Delta\rho H/\rho$ ) along the diffuser tunnel. It can be seen that at this flow the head loss exceeds the Munro head at all risers, so that complete purging should be expected. Because the average slope of the hydraulic grade line is steeper than that of the Munro head, the upstream (first) riser would be easiest to purge while the last riser would be the hardest, everything else being equal. However experiments discussed in the following section clearly showed that, due to the upward sloping configuration of the tunnel soffit, freshwater reached the offtakes of the downstream risers first and hence they purged first. Thus the system geometry dictates that the upstream risers will be the last to purge and it is appropriate to apply the Munro criterion to the first risers. Because the ratio of head loss to Munro head is about 1.07 at the first riser (see Figure 10), the theoretical (Munro) flow for our model becomes

$$Q_M = 19.8/\sqrt{1.07} \approx 19.1 \text{ gpm} = 993 \text{ mgd} \quad (\text{prototype})$$

This flow will be our basis for comparison and evaluation of purging performance in various experiments.

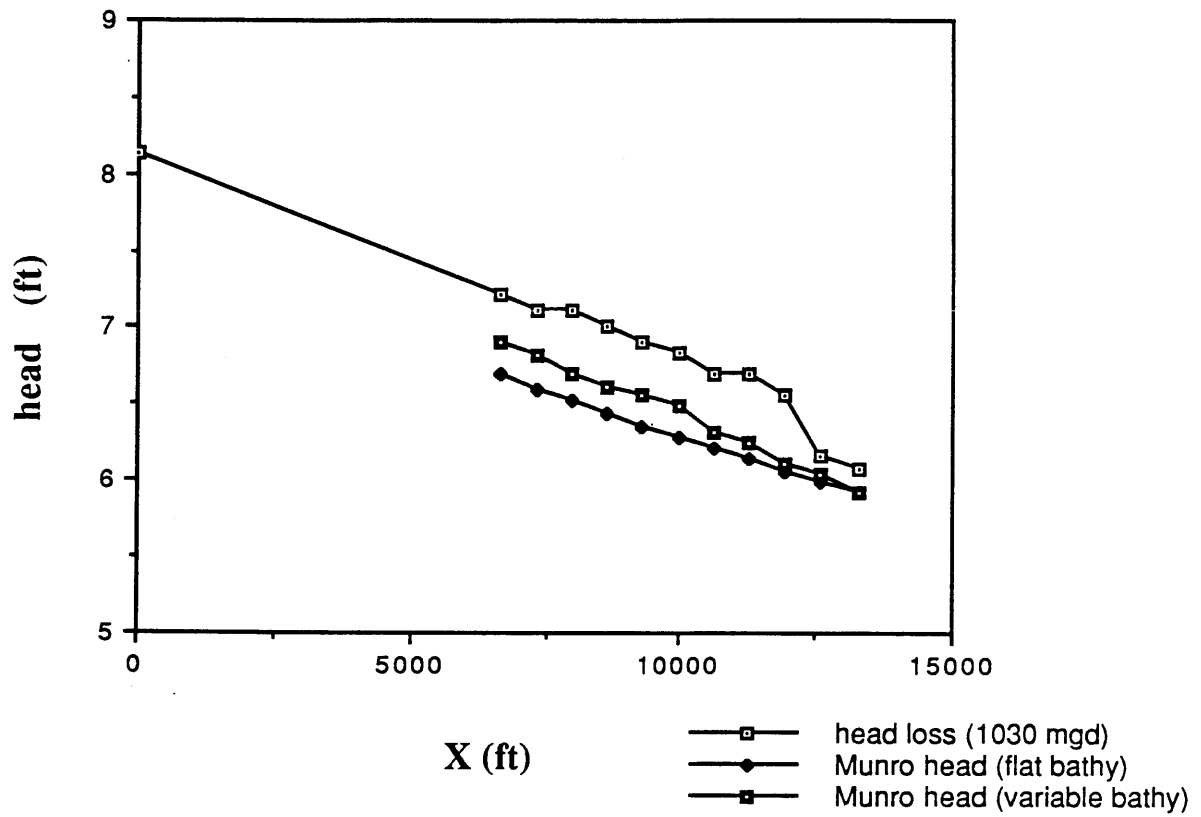


Figure 10 Hydraulic grade line along the section of tunnel modeled (prototype values). Outfall section is from 6600 ft to 132000 ft.

Figure 10 displays the hydraulic grade line over the entire tunnel for a flow of 19.8 gpm (1030 mgd). For the first 60 feet (9900 feet prototype; before the transition to a smaller pipe diameter) the average friction factor is about 0.033 which is a little higher than the value of 0.025 computed for this flow based on the Moody diagram (Figure 4). Note that the experimental value of  $f$  depends on pipe diameter to the fifth power, so small imperfections in material could account for some of the discrepancy. Beyond 60 feet, the rate of headloss increases downstream which is attributed to the decrease in tunnel diameter (and hence hydraulic radius and Reynolds number). Since experiments showed that the downstream section of the tunnel purges first, headloss in the downstream section is less critical to the evaluation of the purging criterion in the model.

## 5.2 Observations during Slowly Varying Flow Conditions

The value of  $Q_M = 19.1$  gpm (993 mgd) is the theoretical (steady) flow at which risers should purge. Observations of tunnel behavior as well as experimental testing of this criterion were conducted as follows. At the beginning of an experiment the system was completely filled with saltwater. This was achieved by recirculating saltwater from the tank through the tunnel and would represent start-up conditions in the prototype tunnel. The flow of freshwater was then started at a rate well below  $Q_M$  and increased slowly in order to have quasi-steady conditions at all times. Because quasi-steady conditions were observed at all times, these tests were termed static tests (also type A tests) and are represented by Hydrograph A sketched schematically in Figure 11.

Observations during these tests showed that the freshwater initially slid over the top of the saltwater wedge and reached the offtakes of the downstream risers first. The first risers to purge were typically in the range of 63-72. Then as the flow

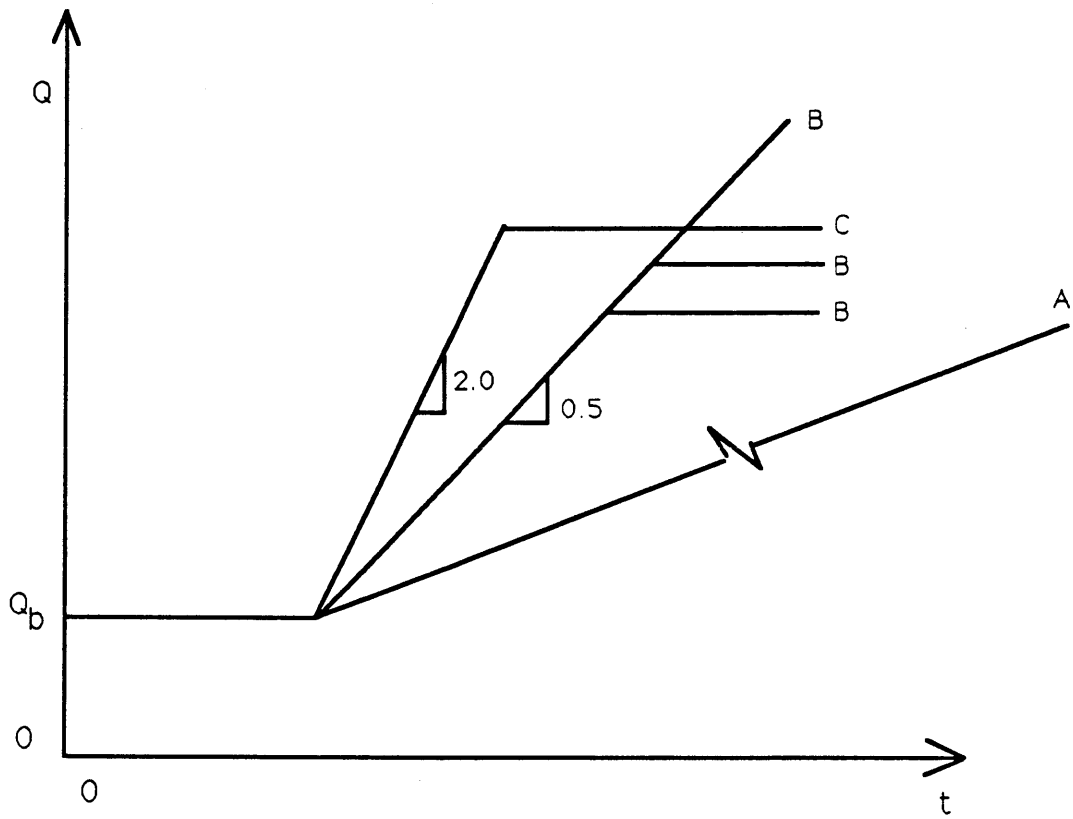


Figure 11 Hydrographs of various tests conducted. In test A flowrate is increased slowly. The slopes in B and C hydrographs are in gpm/sec (model).

increased, all the other end risers (e.g., 73-80) purged as did several risers upstream of the initial set of purged risers. As the flow increased the risers purged sequentially, proceeding backwards, until the first riser purged. There was no strict pattern with regard to the exact sequence of riser purging in repeated experiments. However, the pattern was approximately repeated with the risers close to number 70 being first to purge and riser number 1 being the last.

Theoretically, a riser begins to purge when the internal headloss exceeds the Munro head. In Figure 12  $P_s$  is a reference hydrostatic pressure for a column of saltwater and  $P'_A$  and  $P'_B$  are the actual pressures in the tunnel at the offtakes of adjacent purged and unpurged risers respectively. (If tunnel friction is neglected  $P'_A \simeq P'_B$ .) As the tunnel flow increases (gradually) the tunnel pressure also increases gradually due to the increase in headloss caused by an increasing flow passing through a fixed number of purged risers. Just prior to purging, the internal pressure at the offtake  $P_A \geq P_s$ . However once the riser purges, the pressure  $P'_A$  could drop below  $P_s$  with the riser still flowing upwards. As the effluent flow increases the pressure in the tunnel rises and additional risers purge until  $P'_A \leq P_s$ .

Observations showed that when the diffuser tunnel was partially purged, the unpurged risers were flowing downward with saltwater from the tank. Intrusion occurred through the unpurged risers because the internal headloss was slightly less than the Munro head. In Figure 12, riser B is intruding and therefore  $P'_B < P_s$ . As the effluent flow increases the tunnel pressure increases and additional risers purge again resulting in  $P_s \geq P'_A$  or  $P'_B$ . As each riser purges the pressure drops by a discrete amount and thus it is likely that the head in the tunnel is lower than the Munro head, causing intrusion through unpurged risers. The intrusion through the unpurged risers was relatively slow, as was observed by introducing a contrasting red dye (Rhodamine WT) near the risers ports. Our observations



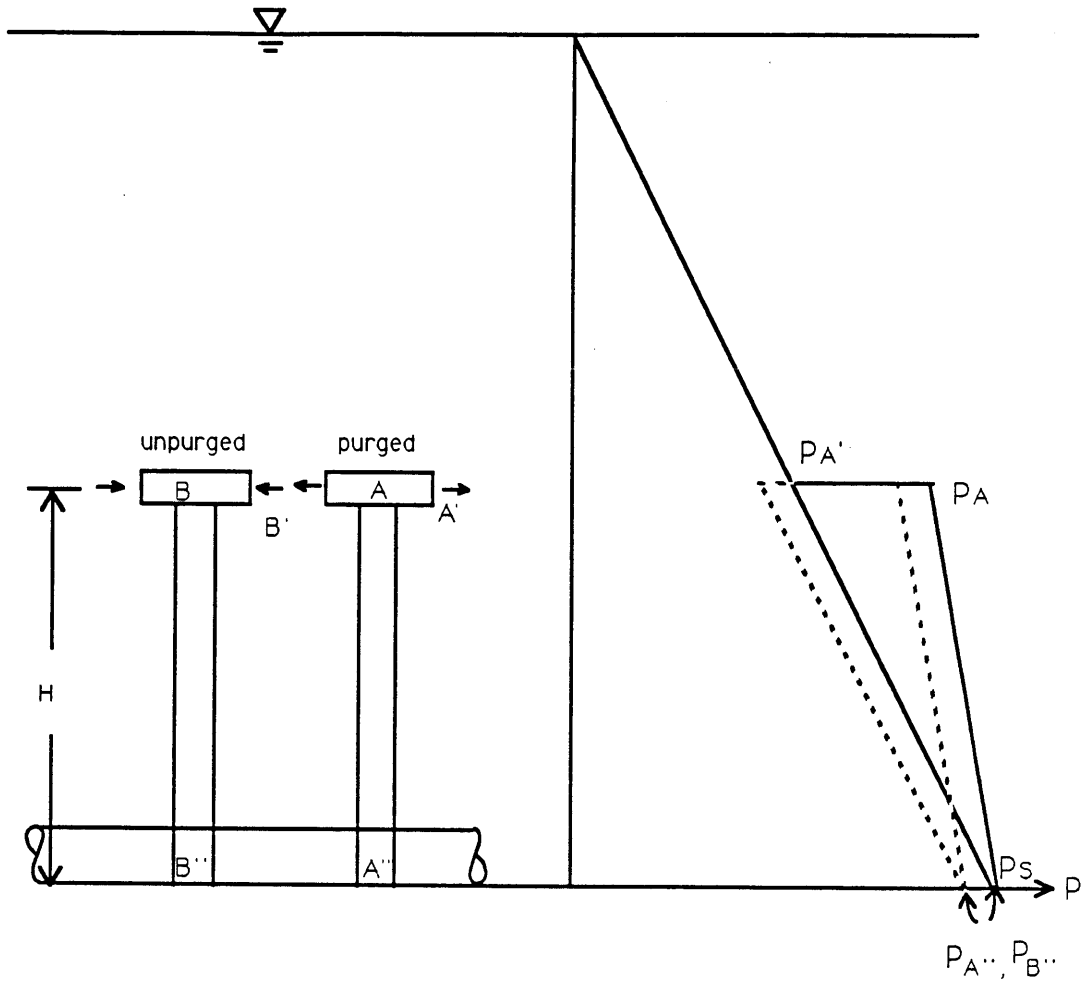


Figure 12 Pressure distribution in purged (A) and unpurged (B) riser.  $P_s$  is the hydrostatic pressure due to saltwater.

showed saltwater intruding at model speeds of 2-10 in/sec. Thus the water in the riser was being continuously replaced with a residence time of between 4 and 20 secs (model) or 1 to 5 minutes (prototype).

Because the ocean tank had a finite volume, its average salinity was progressively diluted during an experiment. Samples of saltwater withdrawn from the tank *at the elevation of the intruding ports* were measured to determine the density of the saltwater in the risers. The observation of downward flow in the unpurged risers gave us confidence that the density in the risers, and hence the relevant density to use in evaluating the Munro criterion, was the same as we measured in the tank. In accordance with Eq. (16), any change in relative density from the target value of  $\Delta\rho/\rho = 0.081$  was used to "correct" the model flowrate. That is, the corrected flow rate was computed from the observed flow rate according to

$$Q_{\text{cor}} = \left[ \frac{.081}{(\Delta\rho/\rho)_{\text{actual}}} \right]^{\frac{1}{2}} Q_{\text{act}} \quad (19)$$

In all of the following, corrected values of flow are reported with no subscript.

Observations showed that the decrease in ocean salinity was monotonic but not constant throughout an experiment. The freshwater plumes from each riser port rose to the top of the tank and overflowed through the drain. In the course of time the lower layers of saltwater also became diluted as the interface between mixed and unmixed receiving water dropped. At the level of the risers, a 5 to 10 percent change in density difference was typical for an average experiment lasting 10-20 minutes. The value of  $\frac{\Delta\rho}{\rho}$  was allowed to decrease to half of its initial value of .081 before additional salt was added.

A static flow test (also referred to as type A test; see Figure 11) showed that the risers were purged at a flow rate of 94% of the Munro flow ( $Q_M = 19.1$  gpm; 993 mgd) or about 930 mgd. See Table 4. Several reasons can be suggested for the fact that the purging flow was slightly below  $Q_M$ . First, head loss associated with the intruding flow would reduce the theoretical head in Eq. (6). Second, mixing takes place at the riser offtakes. This includes both purged risers when there is seawater in the tunnel and unpurged risers where intruding seawater mixes with effluent flow. Such mixing would slightly reduce the density difference seen at unpurged risers making purging easier. Finally, the purging criterion assumes that the flow in the N-1 purged risers equals  $Q/N$ . The difference between use of N and N-1 is about 1%. In the appendix an analysis is presented that takes these factors into consideration. The discussion also considers the numbers of purged and unpurged risers that occur as a function of effluent flow rate (when  $Q_0 < Q_M$ ).

### 5.3 Transient Flow Tests; Sudden Release from the Chlorine-Contact Tanks

The daily averaged effluent flow is expected to vary from 320 mgd to 1270 mgd and instantaneous flows may drop as low as 150 mgd. Clearly there will be extensive periods of time when flow is insufficient to purge the risers based on the above static purging test. However, the water in the chlorine-contact tanks could be used to create the flow necessary to purge the risers. Hence several tests were run simulating dumping of the chlorine-contact tanks.

The volume of the four chlorine-contact tanks is about  $1.8 \times 10^6 \text{ft}^3$  based on a surface area of 75,000  $\text{ft}^2$ , an initial water level of 140.5 ft, and a tank bottom elevation of 117 ft. However, as the water level in the tanks drops below about 124 ft, outflow becomes restricted by a condition of critical flow at the chute entrance; hence the "active" volume is about  $1.2 \times 10^6 \text{ft}^3$ .

Table 4  
Purging Flows in Various Tests

<u>No</u>	<u>Hydrograph type</u>	<u>Bathymetry</u>	<u>Theoretical <math>Q_M</math></u>	<u>Observed <math>Q_{ris}</math></u>	<u><math>\frac{Q_{ris}}{Q_M}</math></u>
<u>Without Venturi</u>					
1	A	uniform	19.1	18.0	0.94
2	B	uniform	19.1	17.6	0.92
3	B	uniform	19.1	16.9	0.88
4	B	uniform	19.1	17.5	0.92
5	B	uniform	19.1	17.6	0.92
6	C	uniform	19.1	17.5	0.92
7	B	non-uniform	19.3	18.9	0.98
8	B	non-uniform	19.3	18.2	0.94
9	B	non-uniform	19.3	18.7	0.97
10	B	non-uniform	19.3	18.9	0.98
<u>With Venturi</u>					
11	A	non-uniform	19.3	17.9	0.93
12	A	non-uniform	19.3	16.9	0.88
13	B	non-uniform	19.3	14.7	0.76
14	B	non-uniform	19.3	13.9	0.72
15	B	non-uniform	19.3	13.4	0.69
16	B	non-uniform	19.3	12.8	0.66

Calculations show that flow rates of up to about 1670 mgd can be obtained with an initial water level of 140.5 ft and a “wide open” gate. However, the time required to achieve this rate depends on the speed of the gate opening. Two types of gate openings have been suggested—a motorized gate and a hydraulic gate. The motorized gate takes about 12 minutes (prototype) to open completely which translates to an average increase in model flow of approximately 0.5 gpm/sec (1.6 mgd/sec in the prototype). The hydraulic gate opens in about 30 seconds (prototype). This is fast enough that the increase in flow rate is limited by gravitational acceleration to an average of about 2 gpm/sec in the model (6.5 mgd/sec in the prototype). Since the hydraulic gate involves higher capital costs and is more difficult to operate, it should have significantly better performance to justify its selection.

Several hydrographs were tested as shown in Figure 11. Hydrographs of type B represent a base flow  $Q_b$  followed by a steady increase associated with dumping the chlorine-contact tanks using a motorized gate. The flow was then leveled off at a constant peak flow and the system was observed until the risers purge. The value of  $Q_b$  was typically 8.5 to 11.5 gpm (440 to 600 mgd). Hydrographs of type C are similar, except they correspond to a hydraulic gate. Hydrograph A is the static flow test, described in the previous section.

5.3.1 Observations of Tunnel Wedge Penetration. The success of a transient purging sequence will depend on the length of the saltwater wedge within the tunnel. The length of the wedge, in turn, will depend on the base flow rate. Our data relating wedge length to steady (base) flow rate are shown in Figure 13. The length of the saltwater wedge did not have an apparent effect on the peak flow rate

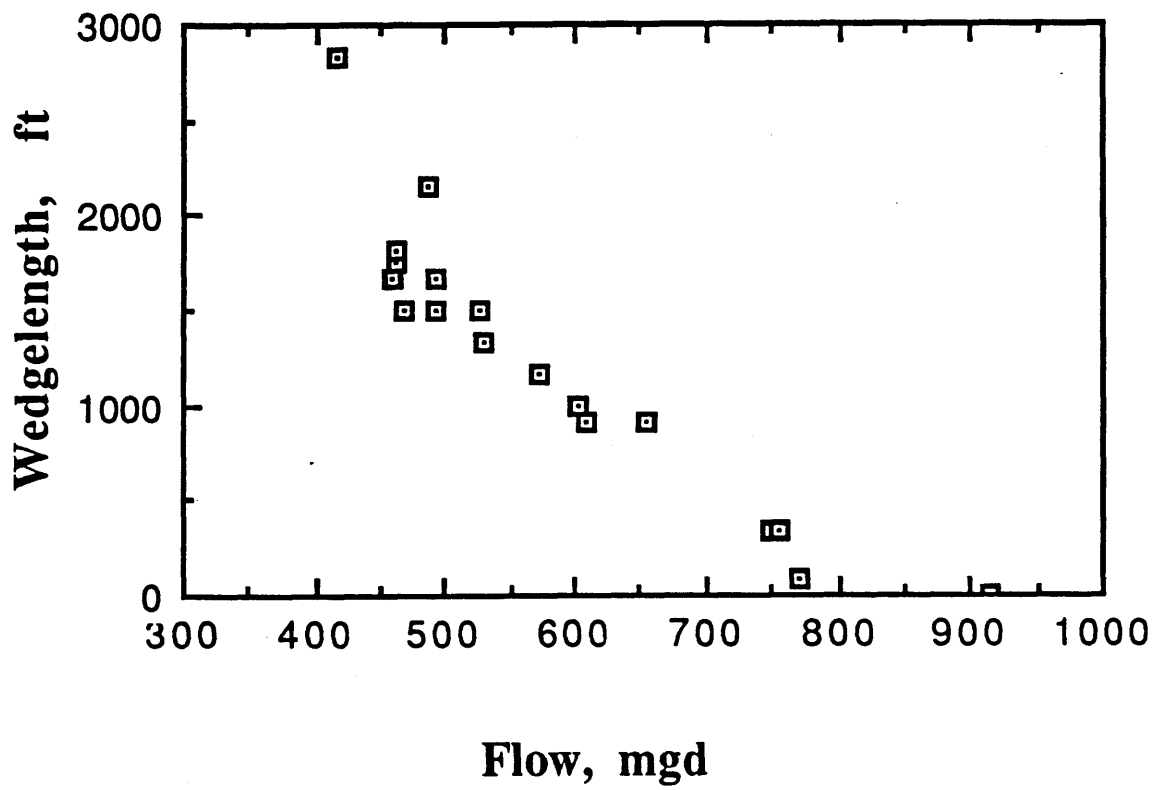


Figure 13 Wedgelen length vs. flowrate

required for purging but, as discussed below, the length had a significant influence on the time required for purging.

Using a value of  $f_m \approx 0.033$ , Eq. (3) gives the theoretical tunnel purge criterion (full pipe flow) as  $Q_{\text{tun}} \approx 6.5$  gpm (340 mgd). Meanwhile, Figure 13 shows that a wedge persists until a flow of about 16 gpm (830 mgd), or approximately 2.5 times the theoretical tunnel purging flow. As discussed in Section 2.2.1, the reason for the high observed purging flow is thought to be the sudden increase in tunnel invert slope which occurs at the beginning of the riser section. In the beginning of the riser section this slope is about 1:240. Indeed exercise of Eq. (3) with a slope of 1:240 gives a theoretical purging flow of 18.8 gpm (980 mgd) for the riser section of the tunnel--in reasonable agreement with our observations. Thus the existence of a penetrating wedge in the tunnel is attributed to the failure to purge saltwater from the *downstream* (riser) section of the tunnel.

Observations show that interfacial mixing within the wedge is intermittent at best. Some mixing must take place in either the tunnel or riser sections as the wedge is being constantly fed by the saltwater from the intruding risers. When the flow increases and the wedge length decreases, the equilibrium wedge configuration is probably established by shear rather than entrainment.

5.3.2 Observations of Purging. In all of the B and C tests, the minimum peak flow rate required to purge the risers (and hence the entire outfall) was similar and ranged from 88-92% of  $Q_M$  (Table 4). These results indicate slightly better purging performance than was observed in the static (A) tests where  $Q_{\text{ris}} \approx 0.94Q_M$ . Because neither rate of flow increase had any observable advantage over the other, it appears that the less expensive motorized gate should be used.

In all tests it was observed that the risers did not purge until salt water in the tunnel was removed.

The results of the B tests show that the excess volume of freshwater (i.e., from the chlorine-contact tanks) required for purging was proportional to the volume of tunnel containing the wedge. Figure 14 plots purging efficiency vs. peak flow rates. The efficiency  $\eta$  is the ratio of the volume of water to be displaced in the tunnel, defined by  $(\pi/4)D^2L_{\text{tun}}$  where  $L_{\text{tun}}$  is the wedge length, to the excess volume of freshwater (obtained from the chlorine-contact tanks) required for purging, defined as the integral over time (until purging) of  $Q - Q_b$ . The results show that the  $\eta$  is around 0.3 to 0.4.

Based on the efficiency  $\eta$  and the base flow it can be determined if the active volume in the chlorine-contact tanks will be sufficient to purge the system. The lower the base flow, the longer is the wedge length  $L_{\text{tun}}$  and the greater is the flow volume generally required from the chlorine-contact tanks. Table 5 summarizes our experimental data and shows that the volume of excess flow necessary to purge the system ranges from about  $4 \times 10^5 \text{ft}^3$  to  $10^6 \text{ft}^3$ , depending on the base flow in the range  $440 < Q_b < 600$  mgd. The active volume of the chlorine-contact tanks is  $1.2 \times 10^6 \text{ft}^3$ . Even at these relatively high base flows the volume of the chlorine-contact tanks was barely enough. At lower base flows the volume would be inadequate. It is concluded that the procedure of dumping the chlorine-contact tanks, as simulated, will be helpful but not always adequate to purge the system. This topic is discussed further in section 5.6



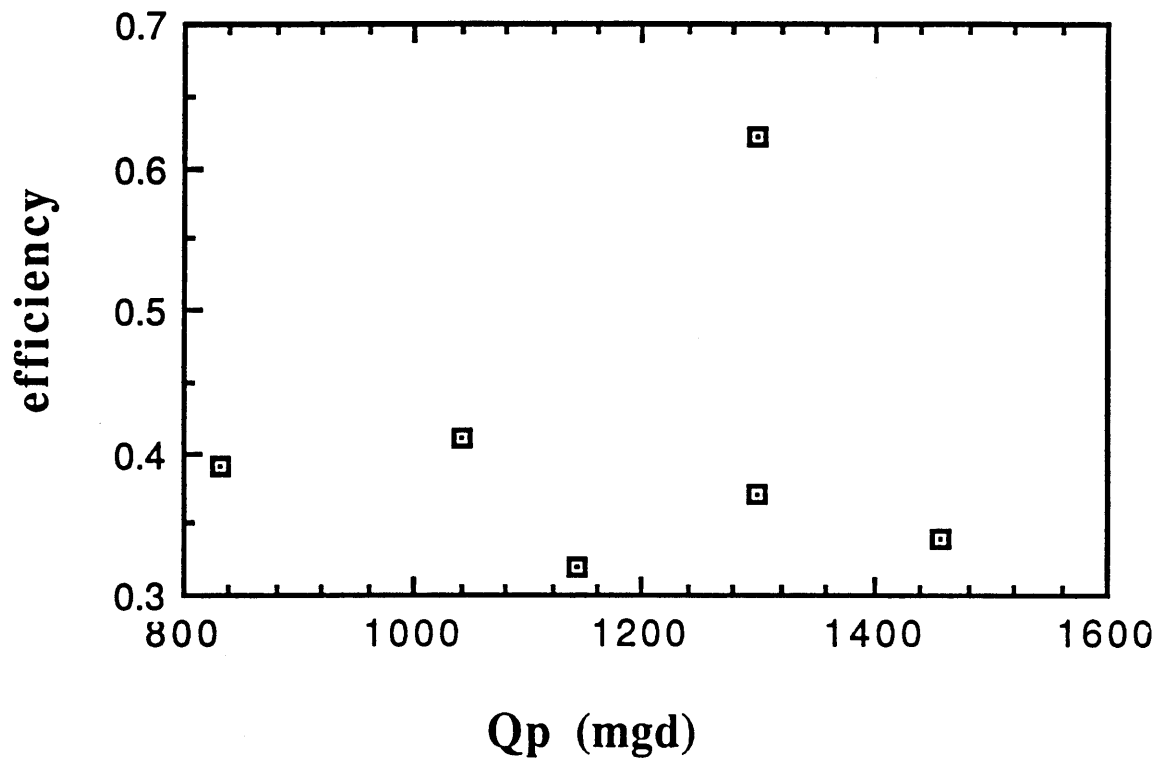


Figure 14 Efficiency of purging vs. peak flow rates.  $Q_{peak}$  is the flow at which the hydrograph is levelled off.

Table 5

Excess Water from Chlorine-Contact Tanks Required for Purging  
as a Function of Hydrograph Parameters  $Q_{\text{base}}$  and  $Q_{\text{peak}}$   
(B tests)

$Q_{\text{base}}$ (mgd)	$Q_{\text{peak}}$ (mgd)	Excess vol. req'd. (ft <sup>3</sup> )	Time req'd (min)
454	1600	$9.8 \times 10^5$	15
604	1520	$5.5 \times 10^5$	11
610	960	$4.1 \times 10^5$	14
573	960	$9.3 \times 10^5$	28
510	1270	$7.0 \times 10^5$	14

#### 5.4 Variable Bathymetry

All tests discussed above were conducted with all diffuser ports at the same elevation. This is equivalent to assuming a flat sea floor with riser caps mounted at a fixed location above the bottom. By contrast, the actual sea floor elevation varies by about 8 feet along the anticipated diffuser location with the upstream risers having the highest elevation (being in shallowest water) and the downstream risers having the lowest elevation. For ease in model construction, bathymetric variability was modeled by increasing the elevation of the upstream risers. The new modeled variation in elevation is shown in Figure 15. Note that this adjustment resulted in a slight increase in *average* riser height.

The change in port elevation may affect both the flow distribution among risers and the theoretical purging criterion (Munro criterion). Assume that each riser would deliver a flow  $q$  which just satisfies the Munro criterion under a condition with constant (average) port elevation. Referring to Figure 16, the flow  $q_i'$  associated with a change in port elevation  $\delta H_i$ , for each riser  $i$ , is

$$q_i' = q \sqrt{\frac{H_i'}{H}} \quad (20a)$$

where

$$H_i' = H + \delta H_i \quad (20b)$$

$H$  is a reference height taken as the distance between port and offtake of the first riser (where the purging criterion is applied). Hence  $H_i'$  is the new elevation difference between port  $i$  and the first riser offtake. For small values of  $\delta H_i/H$ ,

$$q' \simeq q \left[ 1 + \frac{\delta H}{2H} \right] \quad (20c)$$

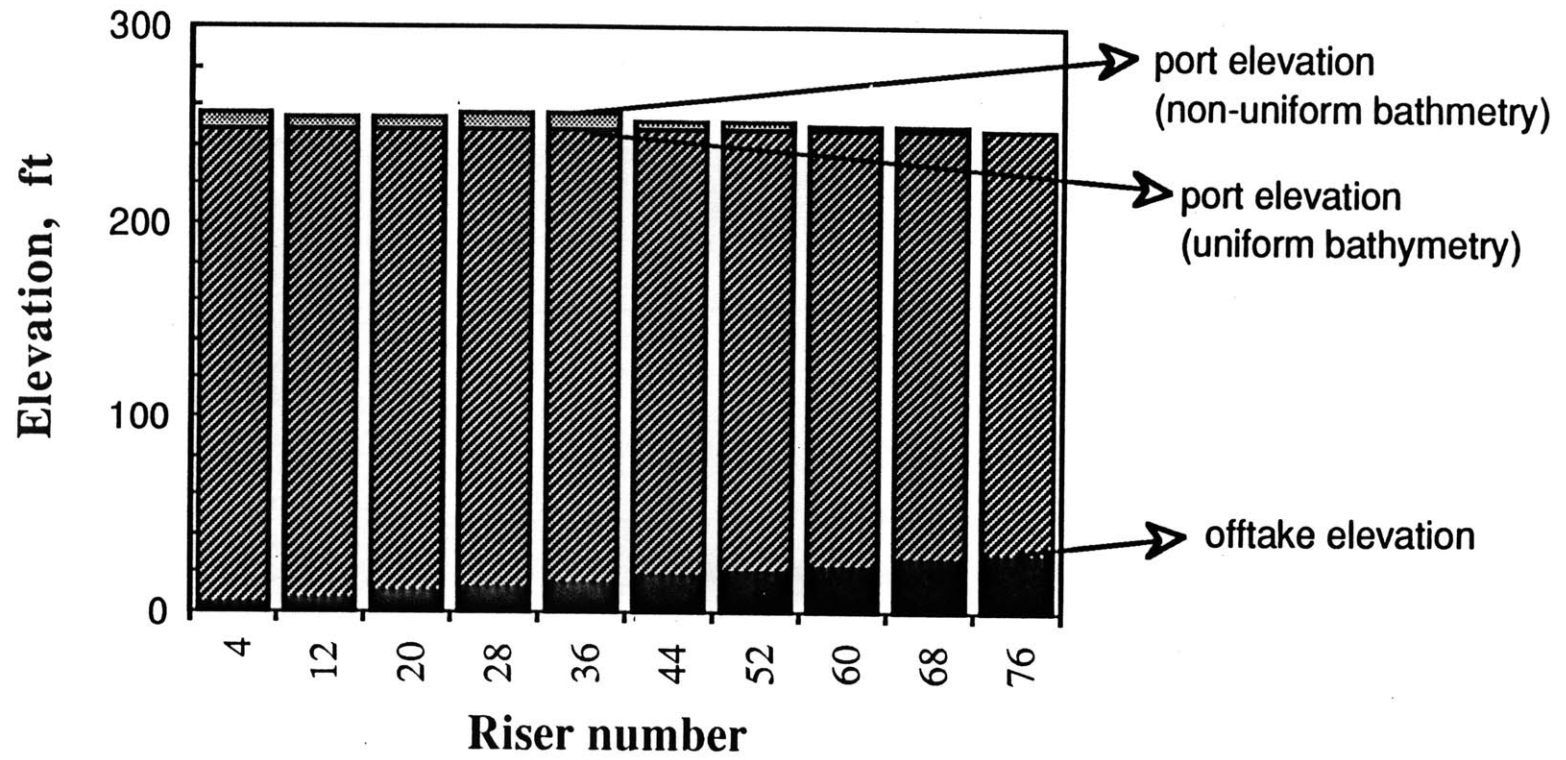


Figure 15 Riser elevation

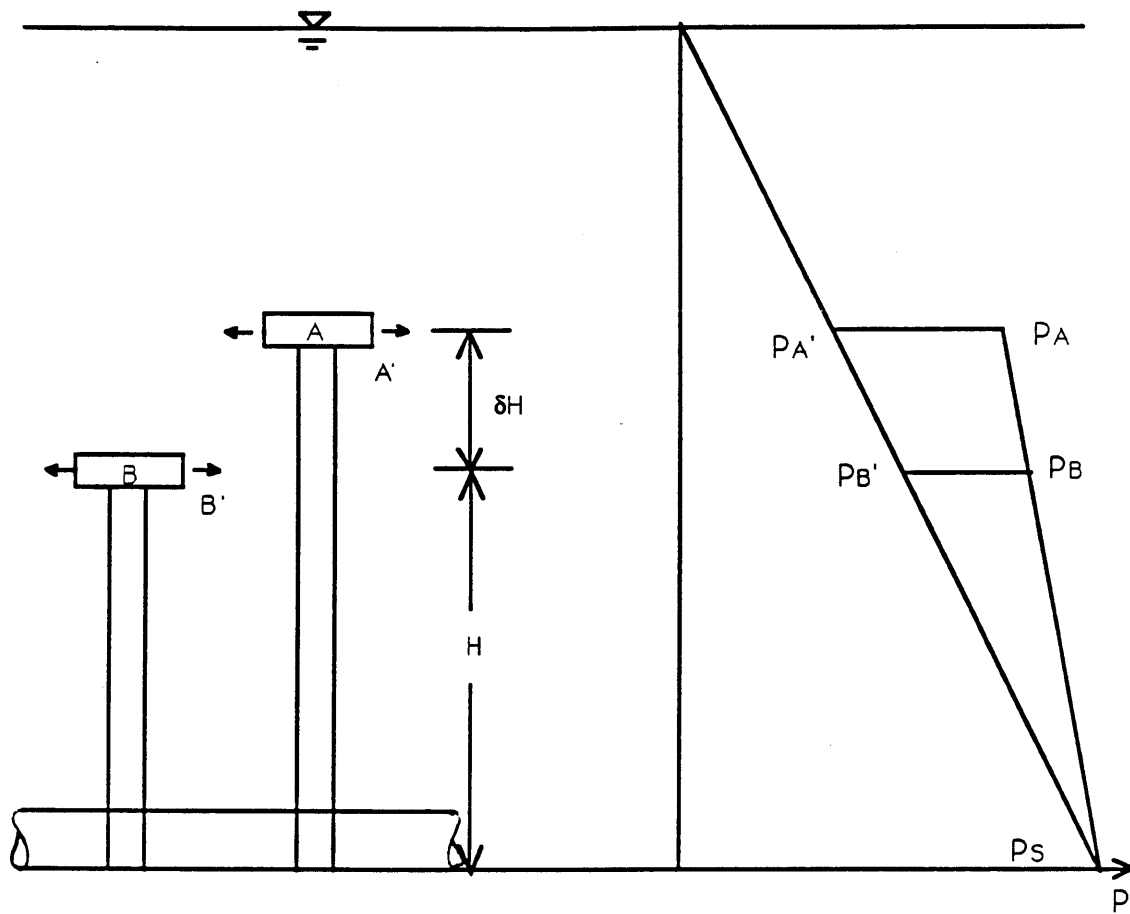


Figure 16 Pressure distribution in non-uniform riser elevation

or the change in flow  $\delta q_i$  is

$$\delta q_i \approx q_i \frac{\delta H_i}{2H} \quad (20d)$$

The total change in flow is the sum of  $\delta q_i$  over all the risers which, with the linearization assumption, is zero. Hence for small elevation changes, with no average change, flow will increase in the higher (upstream) riser and decrease in the lower (downstream) riser in proportion to the respective elevation change. There is no change in net flow, of course, since the total effluent flow is given.

The tunnel slope still dictates that the upstream risers will be the last to purge which requires that the tunnel head exceed the differential hydrostatic head (Munro head) at this point. Since the Munro head is proportional to the (first) riser height, the Munro criterion is satisfied when

$$q_1' = q_1 \sqrt{\frac{H_1'}{H}} \quad (21)$$

which is identical to Eq. (20a) for the first riser. Hence an increase in the elevation of the upstream risers with a compensating decrease in the elevation of the downstream risers increases both the relative flow through the upstream risers and the required purging flow to the same degree. As a result, there is no change in the "system Munro flow" for the case of variable port elevation in comparison with the case of constant (average) port elevation.

In our model geometry (Figure 16), the average port elevation was increased such that the Munro flow became 19.3 gpm (1004 mgd). Observations showed that purging with the non-uniform bathymetry occurred for flows in the range from 18.2

to 18.9 gpm or about 94 to 98% of the new  $Q_M$ . The values of the purging flows are summarized in Table 4 and compared to previous values for uniform bathymetry. One can conclude that non-uniform bathymetry has a slight adverse effect on diffuser purging performance judging by the ratio of observed to theoretical purging flow. However all the observed purging flows are still less than the theoretical values.

### 5.5 Riser Intrusion

Some limited tests were performed to observe the intrusion of seawater into the risers at low flow. Before describing these tests, however, it must be emphasized that the model riser caps were designed to properly simulate head loss and hence the required purging flow, but not necessarily the correct intrusion. For example, a 2-port riser cap was used in the model to represent an 8-port cap (with similar head loss) in the prototype. Hence, everything else being equal, the model port diameter would be larger than scale by a factor of about 2. Because riser intrusion is expected to depend on a port Froude number which, *for a given port velocity*, is inversely proportional to the square root of port diameter (see Eq. (1)), we would expect to find intrusion beginning at a flow rate of  $\sqrt{2}$  or 1.41 times higher in the model than in the prototype. Furthermore, as discussed in section 4.2, the calibrated model port diameter turned out to be another 11% larger than prototype in order to achieve the same head loss. Because the port Froude number varies inversely as the port diameter to the 5/2 power *for a given port flow rate*, the critical intrusion flow would be another  $1.11^{5/2} \approx 1.30$  times higher, or a total of about  $1.41 \times 1.30 = 1.84$  times higher, in the model than in the prototype.

The intrusion tests were carried out with adjusted (non-uniform) diffuser port elevations. Tests were begun under conditions with all risers purged and a low flow

rate that was reduced slowly (to avoid any inertial effect) until intrusion was observed. In all cases either riser number 80 or 79 (at the downstream end) intruded first. This is to be expected for two reasons. First, the last 8 riser caps have the lowest elevation. As discussed previously, the upward freshwater flow in these risers with least elevation is less than in the remaining risers due to the lower buoyancy effect (draft). Second, since riser number 80 is the last riser at the downstream end, the dynamic pressure in the tunnel is lower at point B' than at A' due to friction losses. So in Figure 17  $P_A > P_B$ . This causes higher upward flow in the riser at A' than the one at B'. Thus  $F_{0A} > F_{0B}$ . So riser 80 has the lowest port Froude number and intrudes first. Once one riser experiences (downward) intrusion, the salt water enters the tunnel, mixes with freshwater, and flows up the adjacent risers that are already flowing up. This causes the density to rise in the column and thus the excess hydrostatic pressure increases. And since the dynamic pressure in the tunnel is low at this low flow rate,  $h_L \ll \frac{\Delta\rho}{\rho}gh$  and the riser quickly becomes unpurged, with downward flow. Further analysis of riser intrusion where the diffuser is not fully purged is presented in the appendix.

Observations from a number of tests showed that seawater first began to intrude at a flow rate of 1.1 to 1.4 gpm. *Assuming uniform flow through each riser*, this corresponds to port Froude numbers of .88 to 1.12 or somewhat higher than the value of about 0.7 expected for a single horizontal port (Wilkinson, 1988a). Of course part of the explanation for the higher Froude number lies in the fact that the riser flows are not equal and that intrusion is observed first in the downstream riser with least flow. Scaling up to prototype, for 80 risers each with eight ports of 0.42-ft diameter, the range of  $F_0$  from 0.9 to 1.1 corresponds to prototype flows of 31 to 38 mgd, or safely below any normal base flow. The range of 31 to 38 mgd can



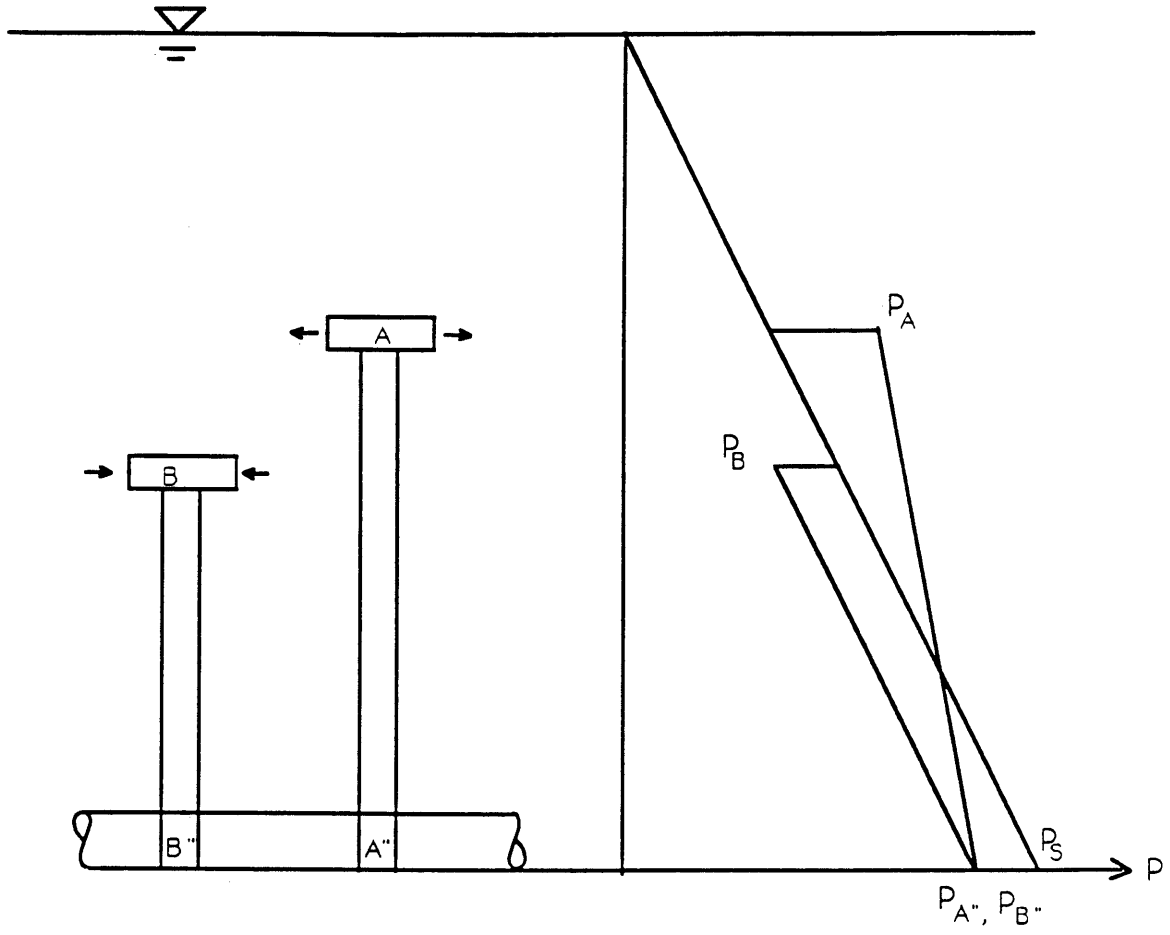


Figure 17 Pressure distribution during intrusion

also be calculated by multiplying the observed model range of 1.1 to 1.4 gpm by the flow rate ratio of 36000 and dividing by the factor 1.84 discussed above.

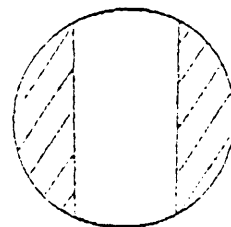
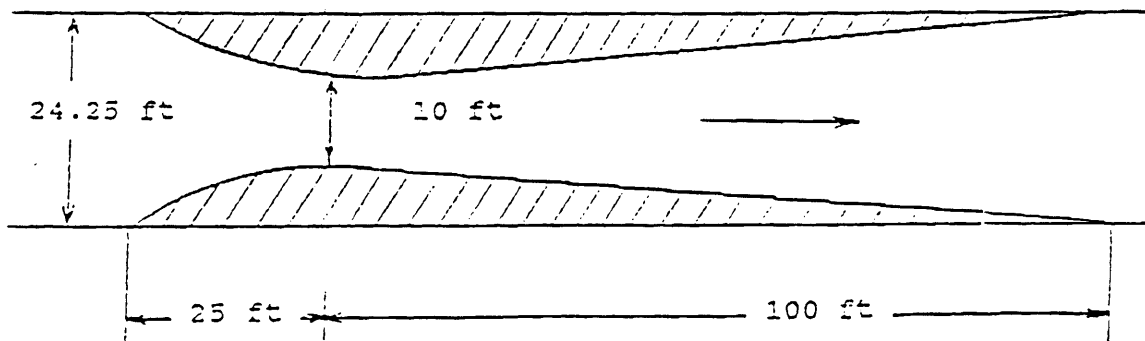
The above observations pertain to conditions of steady very low flow which results in initial intrusion into the *offshore* risers. It should be apparent that this contrasts with conditions of a sudden flow shutdown where inertial effects (as discussed in Section 2.2.3 in connection with circulation blocking) cause the *shoreward* risers to intrude first. This latter type of intrusion was observed in the model under all flow rates whenever the system was suddenly shut down.

### 5.6 Tests with Venturi Section

In order for the rapid purging scheme to work, the saltwater wedge in the tunnel needs to be removed first. While the experimental results of Section 5.3 indicated that the flow rate required to purge the tunnel was somewhat less than that required to purge the risers, the time scale of the former is much greater. Thus a larger volume of excess flow (i.e., from the chlorine-contact tanks) would be required to purge the saltwater wedge.

In an attempt to reduce upstream saltwater penetration, a lateral constriction in the form of a Venturi section was installed just upstream of the first riser. Figure 18 shows the shape of the Venturi. The width of the Venturi at its narrowest point (throat) is 10 feet and the cross-sectional area is about 236 ft<sup>2</sup> or about 51% of the upstream cross-sectional area of 464 ft<sup>2</sup>. The contraction takes place over a distance of 25 feet which translates to 1.8 inches in the model. The Venturi is not expected to impose any significant headloss on the tunnel.

Experiments indicated that the minimum flow (below which saltwater penetration upstream of the Venturi was observed) was about  $Q = 6.5$  gpm



Section at Throat

Figure 18 Shape of Venturi

(340 mgd). As discussed in Section 2.2.1, the success of the Venturi in reducing upstream seawater penetration can be explained in terms of hydraulic control near the Venturi throat. Treating the constriction as a rectangle with width B equal to 10' and height H = 23.6', the value of  $F_c$  from Eq. (4) is 0.49, which is somewhat smaller than the value of 0.58 expected for a vertical-walled channel with 50% contraction (see Section 2.2.1).

A more precise theoretical calculation can be made that considers the circular cross-section of the tunnel upstream of the constriction. If the saltwater wedge is arrested in the Venturi section, the densimetric hydraulic grade line can be evaluated in terms of the upper layer (effluent) depth (y) and velocity (u). Using subscript 1 for conditions upstream of the constriction and subscript c for conditions at the constriction, and assuming no energy loss in the contraction,

$$y_1 + \frac{u_1^2}{2g'} = y_c + \frac{u_c^2}{2g'} \quad (22)$$

Critical flow at the constriction requires  $y_c = u_c^2/g'$  and the minimum flow for which the wedge is arrested by the contraction occurs when  $y_1 = D$ . Expressing  $u_1$  and  $u_c$  in terms of Q and their respective cross-sectional areas, Eq. (22) becomes

$$D + \frac{8Q^2}{\pi^2 g' D^4} = \frac{3Q^{2/3}}{2B^{2/3} g'^{1/3}} \quad (23)$$

Solving Eq. (23) with D = 24.3 feet, B = 10 feet, and  $g' = (32.2)(.027) = 0.87 \text{ ft/s}^2$  yields Q = 421 mgd. The corresponding densimetric Froude number, evaluated from Eq. (4), is  $F_c = 0.61$

The experimental values (Q = 340 mgd,  $F_c = 0.49$ ) are about 20% smaller than the theoretical values. The differences may be attributed to mixing (described

below) which lowers the effective value of  $\Delta\rho/\rho$ . A base flow of 340 mgd, which is near the design daily average low flow of 320 mgd, will normally be available so the wedge will be absent from the tunnel most of the time.

Observations for flows at or above 340 mgd showed that saltwater from the riser section of the outfall was arrested within the Venturi section. Considerable shear mixing was observed in the downstream expansion section of the Venturi.

Type A (static) tests were carried out with the Venturi installed and a base flow somewhat larger than necessary to purge the tunnel. As in previous tests without the Venturi, some of the risers at the downstream end of the riser section were purged at this base flow. As the flow was increased slowly, not only more downstream risers but also the first few upstream risers were purged. Purging of the first few risers was attributed to mixing induced by the Venturi just upstream. Some of the mixed water with intermediate density entered the initial risers, reducing the hydrostatic head and enabled the dynamic head in the tunnel to push the water upwards. Hence with the Venturi, the last risers to purge were in the middle, typically around number 20. The observed system purging flow ranged from 16.9 to 17.9 gpm (880 to 930 mgd) or about 88 to 93% of  $Q_M$ . This represents a slight improvement over the case without the Venturi.

Type B (rapid purge) tests were also conducted starting with a sufficient base flow to purge the tunnel, and then increasing flow at 0.5 gpm/s (1.6 mgd/s). In these tests, the downstream risers again purged first. As soon as the flow increased over  $0.66Q_M - 0.70Q_M$ , the rest of the remaining ten to twenty upstream risers started to flow upwards. If the flow was leveled off at this point ( $\geq 0.66Q_M$ ) the risers purged after a short time characterized by the residence time within the riser (5 to 10 seconds in the model; 2 to 3 minutes in the prototype).

However, if the flow was reduced to less than about  $0.65Q_M$  even after all the risers were flowing up, but before they were completely purged, some of the risers reverted to downward flow and remained unpurged. This occurred because some of the risers were flowing with a mixture of seawater and freshwater, and hence with densities greater than that of freshwater. Hence, the Munro head exceeded the dynamic head. Furthermore, as the flow was reduced and as most of the risers continued to flow upwards, some of the upstream risers purged completely. This increased the flow in these risers and thus reduced the flow in the unpurged but mixed risers. The dynamic head available in the tunnel dropped for these downstream risers such that  $h_L < \Delta\rho H/\rho$ . Resulting downward flow brought in denser saltwater—further stabilizing the unpurged state.

With the Venturi, the purging flow ( $\approx 0.7Q_M$ ) was significantly less than with no Venturi. We believe this is because of the decreased inventory of salt water in the tunnel due to the absence of an upstream wedge. This condition, in turn, enables a *set of risers to purge simultaneously*. In analogy with Eq. (6), the riser purging flow might then be given by

$$Q_{ris} = (N - j) \sqrt{\frac{\Delta\rho H}{\alpha\rho}} \quad (24)$$

where  $j$  (usually  $10 < j < 20$ ) is the number of risers purging simultaneously. Hence the flow required is less than  $Q_M$ .

The lower purging flow, along with the absence of an extended saltwater wedge, reduces the excess volume of water required to achieve purging. Table 6 gives the amount of water from the chlorine-contact tanks required to purge the system in various Type B tests. In all cases, the required volume is at least a factor of two

Table 6

Excess Water from Chlorine-Contact Tanks Required for Purging with Venturi Section as a Function of Hydrograph Parameters  $Q_{\text{base}}$  and  $Q_{\text{peak}}$  (B tests)

$Q_{\text{base}}$ (mgd)	$Q_{\text{peak}}$ (mgd)	Excess vol. req'd. (ft <sup>3</sup> )	Time req'd (min)
390	840	$5.3 \times 10^5$	15
416	765	$6.2 \times 10^5$	21
420	725	$4.3 \times 10^5$	17
380	700	$4.3 \times 10^5$	16
504	1341	$5.5 \times 10^5$	11
470	1220	$3.8 \times 10^5$	9

less than the active volume of the chlorine-contact tanks. Hence we conclude that, with the Venturi section installed and for conditions with no upstream seawater penetration in the tunnel ( $Q \geq 340$  mgd), the system may be purged by intermittent dumping of the chlorine-contact tanks achieved by opening a motorized gate.

## 6 SUMMARY AND CONCLUSIONS

This report describes a hydraulic scale model of the Boston Wastewater Tunnel. Nominal scale ratios (prototype to model) include

Froude number	1:1
diameter and heights	83:1
friction	1:2
slopes	1:2
lengths	166:1
density differences	1:3
Reynolds numbers	440:1
flow rates	36000:1
times	16:1 (risers)
	32:1 (tunnel)

Because the prototype design was not finalized at the time of model construction (indeed the final design was selected, in part, on our model results), the model was designed based largely on the earlier STFP study (MWRA, 1988). As such it was expected to *resemble* the ultimate prototype design. Our philosophy was thus to study purging phenomena in the model and then translate this *understanding* into the prototype design. The major observations and conclusions of the study are summarized below.



## 6.1 Basic Observations

- During start-up with low to moderate flows (up to at least 1000 mgd) observations showed the freshwater wedge advancing downstream along the tunnel soffit. Due to the upward slope of the tunnel, the downstream risers (with highest offtake elevation) purged first.
- If the flow rate was insufficient to purge all risers, the upstream risers as a block remained unpurged. Saltwater was observed to intrude *downward* through unpurged risers at a rate up to about 4 ft/s (prototype). In between the purged and unpurged risers several risers exhibited exchange flow and/or mixed upward flow.
- As flow rate increased, additional risers purged, working backwards. Riser 1 (furthest upstream) was consistently the last to purge. Thus the theoretical purging criterion (Munro criterion) should be based on Riser 1.
- Measurements of hydraulic grade line (made with freshwater) showed that the internal head equaled the excess hydrostatic head at Riser 1 at a prototype flow of about 995 mgd. This is the basic Munro flow,  $Q_M$ . At this flow, the internal head loss at all downstream risers was slightly less than the corresponding excess hydrostatic head, or Munro head, making Riser 1 the “easiest last riser to purge.” The fact that tunnel geometry dictates that it is in fact the last riser to purge indicates good design.
- Hydraulic grade line measurements also indicated a tunnel friction factor in the model of  $f \simeq 0.033$  at a prototype flow rate of 1030 mgd. Model scaling was based on a friction factor ratio of 0.5 implying our model corresponded to a prototype friction factor of about 0.016, which is representative of relatively old pipe

conditions. The tunnel purge criterion (condition of full pipe flow) for this value of  $f$  is 340 mgd.

- When flow was increased very slowly (referred to as a static purge test), purging occurred at a flow rate of around 94% of  $Q_M$ .
- Salt water penetration within the tunnel upstream of the riser section depended on flow rate and persisted at flow rates up to about 830 mgd which is nearly 2.5 times the tunnel purging criterion referenced above and about 80% of the observed riser purging flow. The reason for the much higher observed tunnel purging flow is the increase in tunnel invert slope which occurs downstream in the riser section

## 6.2 Tests Simulating the Dumping of Chlorine-Contact Tanks

- Rapid purging tests (which simulate a temporary increase in flow due to discharge from chlorine-contact tanks) were conducted by using generic hydrographs characterized by a constant base flow, followed by increasing flow at a fixed rate of increase, followed by a constant peak flow. Two rates of increase in flow were chosen: one of 1.6 mgd/sec, characteristic of a motorized gate, and the second of 6.5 mgd/sec, which represents the computed acceleration of flow in the tunnel (which would govern the rate of increase if a hydraulic gate were used). Of interest in these tests was the peak flow, the required time, and especially the total excess volume required for purging.
- The minimum peak flow at which purging occurred was in the range of 88-92% of  $Q_M$  which is similar to the static tests. No difference was observed between tests with a motorized gate and a hydraulic gate.

- Rapid purging requires the displacement of salt (and overlying fresh) water in the tunnel. The efficiency of displacement (i.e., volume of salt and overlying fresh water divided by the excess volume of water released by the time purging occurred) ranged generally between about 30% and 40%.
- The success of rapid purging thus depended strongly on the base flow rate. The volume of excess flow required for purging became comparable with the active volume of the chlorine-contact tanks at a base flow of around 500 mgd. Because this flow rate is greater than most dry weather flows, there was a strong incentive to explore ways to reduce tunnel intrusion (i.e., through use of a Venturi).

### 6.3 Sensitivity to Variable Bathymetry

- With the tentative alignment chosen for the diffuser, water depths (and hence riser port elevations) vary by about 8 ft over the length of the diffuser. Model tests of both static and rapid purging showed no significant sensitivity to bathymetry in this range.

### 6.4 Venturi

- To attempt to limit sea water penetration in the tunnel a “Venturi section” was installed just upstream of the first riser. The Venturi consisted of a lateral constriction with throat width of 10 feet. In general, the Venturi substantially reduced tunnel intrusion. The wedge was eliminated for flows greater than about 340 mgd which corresponds to the original tunnel purging criterion based on full pipe flow.

- Theoretical calculations, based on a condition of densimetric critical flow at the throat and assuming no mixing indicate that the wedge should be expelled at a flow of about 420 mgd. The lesser observed flow is attributed to mixing downstream from the Venturi.
- Substantial interfacial mixing was observed downstream from the Venturi. In addition to helping decrease the effective tunnel purging flow, this mixing facilitates purging of the upstream risers with the result that "middle risers" (typically numbers 10-30) were the last to purge.
- The flow required for static purging with the Venturi was between 88-93% of  $Q_M$ , which is similar to observations without the Venturi.
- On the other hand rapid purging was greatly improved. Beginning with a base flow of about 400 mgd (no tunnel wedge), purging occurred at peak flows as low as 66% of  $Q_M$ . The time required for purging was 10 to 20 minutes and the excess volume of water required was always less than about  $6 \times 10^5 \text{ft}^3$  or 50% of the active volume within the chlorine-contact tanks. It is therefore concluded that a tunnel design which includes the Venturi section and provisions to dump the chlorine-contact tanks using a motorized gate will be successful at purging seawater from the outfall, *during conditions with no tunnel wedge*. Theory says this will occur at a base flow of 420 mgd, but observations suggest it will occur at flows down to 340 mgd. Based on the success of rapid purging without the Venturi, *under conditions with wedge lengths up to about 1500 ft* rapid purging with the Venturi should be successful at flow rates even lower than 340 mgd, but confirmatory experiments were not performed.

## 6.5 Salt Water Intrusion through Ports

- Although the model was not designed to look at riser intrusion, some exploratory observations were made. Intrusion was always observed to begin in either the last or the next-to-last riser (numbers 79 or 80) and began at a port Froude number (based on the port diameter and an assumed port flow rate of 1/160 of the total flow) of about 0.9 to 1.1, which is a little higher than the value of 0.7 expected for a single horizontal port. The explanation may be due, in part, to a non-uniform riser flow distributions yielding proportionally less flow through the downstream risers. Scaling up to prototype, for 80 risers each with eight ports of 0.42-ft diameter, the observed critical value of  $F_0 = 1.1$  corresponds to a prototype flow of about 38 mgd, or safely below any normal base flow. However, because actual discharge ports will have different geometry, and will not all be of equal size (downstream risers will have larger ports), caution is urged in using our model results to evaluate riser intrusion.

## 7 REFERENCES

- Armi, L., D. M. Farmer. 1986. Maximal two-layer exchange through a contraction with barotropic flow. *Journal of Fluid Mech.* 164:27-51.
- Bennet, N. J. 1981. Initial dilution: A practical study on the Hastings Long Sea outfalls. Proceedings, ICE, Vol. 70.
- Brooks, N. H. 1970. Conceptual design of submarine outfalls, II: Hydraulic design of diffusers. Tech Memo 70-2, M. W. Keck Laboratory of Hydraulics and Water Resources, California Institute of Technology, Pasadena, Calif.
- Brooks, N. H. 1988. Seawater intrusion and purging in tunneled outfalls: A case of multiple flow states. *Schweizer Ingenieur und Architekt* 6:156-160.
- Charlton, J. A. 1982. Hydraulic modeling of saline intrusion into sea outfalls. Proceedings, International Conference on the Hydraulic Modeling of Civil Engineering Structures, Coventry, England. 349-356.
- Massachusetts Water Resources Authority. 1988. Secondary treatment facilities plan, Vol. 5: Effluent outfall. Final Report.
- Munro, D. 1981. Seawater exclusion from tunneled outfall discharge sewage. Report 7-M, Water Research Centre, Stevenage Laboratory.

- Roberts, P. J. W. 1989. Dilution hydraulic model study of the Boston wastewater outfall. Report No. SCEGIT 89-101, Georgia Inst. of Techn., School of Civil Engineering, Atlanta, Ga.
- Streeter, V. L., E. B. Wylie. *Fluid mechanics*. 7th ed., McGraw-Hill.
- Wilkinson, D. L. 1985. Seawater circulation in sewage outfall tunnels. *Journal of Hydraulic Engineering, ASCE* 111(HY5):846-858.
- Wilkinson, D. L. 1988a. Avoidance of seawater intrusion into ports of ocean outfall. *Journal of Hydraulic Engineering, ASCE* 114(2):218-228.
- Wilkinson, D. L. 1988b. Hydraulic modeling of tunneled outfalls. Proc. Int'l Conf. on Marine Disposal of Wastewater, Wellington, New Zealand.

## Appendix SEAWATER INTRUSION IN A PARTIALLY PURGED DIFFUSER

Consider a start-up condition where the diffuser and tunnel are initially filled with saltwater. Effluent flow then commences. In an ideal case of a horizontal diffuser with plug flow, where the freshwater-saltwater interface is vertical, effluent reaches one riser offtake at a time. In this case considerations leading to the Munro criterion defined earlier can be used to compute the number of purged risers under partially purged conditions. In analogy with Eq. (6), the number of purged risers,  $N - j$ , is proportional to the effluent flow or

$$\frac{N-j}{N} = \frac{Q_0}{Q_M} \quad (\text{A.1})$$

In Figure A.1 this linear relationship is described by the solid "equivalence" line.

However, at the moderate effluent flow rates that generally prevail, the freshwater wedge slides over the saltwater. This freshwater layer has a finite thickness and reaches the downstream risers first due to the upward slope of the tunnel soffit (see Figure 3). Sets of riser offtakes at similar elevations gain access to the freshwater simultaneously and purge together. This explanation was used in the text to help explain why the effluent flow  $Q_{\text{ris}}$  required for riser purging was somewhat less than  $Q_M$ . If we assume that the same process takes place in a partially purged diffuser, then we should expect that

$$\frac{N-j}{N} \geq \frac{Q_0}{Q_M} \quad (\text{A.2})$$

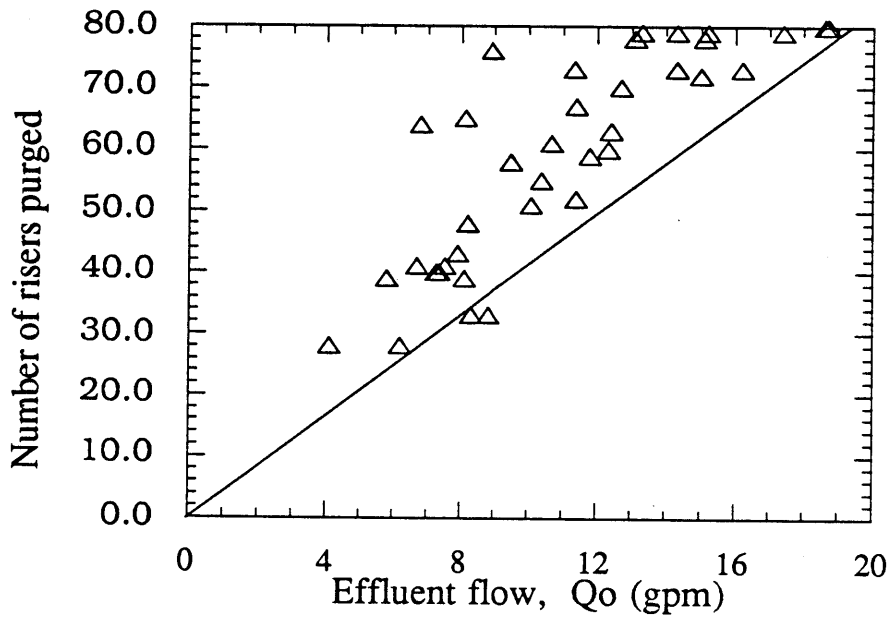


Figure A1 Number of purged risers,  $N-j$ , as a function of normalized effluent flow rate



Hence Eq. (A.1) can be expected to describe the maximum number of unpurged risers  $j_{\max}$ . Figure A.1 presents experimental data on the number of purged risers for a range of partially purged conditions. These riser purging data are in qualitative agreement with Eq. (A.2), with nearly all lying above the equivalence line.

Additionally, as mentioned in the text, the finite number of risers causes the pressure in the tunnel to drop by discrete amounts as each additional or each set of additional risers purge. Thus the tunnel pressure is usually likely to be below the Munro pressure.

The above two effects cause a downflow in the unpurged risers since the pressure in the tunnel falls below the Munro pressure. This results in headlosses of

$$h_d = \alpha_d q_d^2 \quad (A.3)$$

in the unpurged risers and

$$h_u = \alpha_u q_u^2 \quad (A.4)$$

in the purged risers. Here  $q_d$  is the downflow in each riser and  $\alpha_d$  is a dimensional headloss coefficient in the unpurged risers.  $q_u$  is upflow in each riser and  $\alpha_u$  is the corresponding headloss coefficient in the purged risers. We assume that  $q_u$  and  $q_d$  are equal for all purged and unpurged risers respectively.

The total downflow in all unpurged risers is

$$Q_d = j q_d \quad (A.5)$$

The total upflow in all purged risers is

$$Q_u = (N - j)q_u = Q_0 + Q_d \quad (\text{A.6})$$

where  $j$  is the number of unpurged risers,  $N - j$  is the number of purged risers, and  $Q_0$  is the effluent flow.

As observed in the tests (especially those without a Venturi) we will assume that the unpurged risers are located upstream and that the intruding saltwater mixes uniformly with the effluent flow in the diffuser section of the tunnel downstream. Thus fluid in the downstream purged risers has a density  $\rho_{ave}$  slightly greater than freshwater,

$$\rho_{ave} = \frac{\rho Q_0 + \rho_s Q_d}{Q_0 + Q_d} \quad (\text{A.7})$$

A modified purging criterion that takes into account both headloss and mixing associated with the downflow is found by equating the tunnel pressure head to the reduced Munro head  $\Delta\rho' H/\rho$ . Referring to Figure A.2, this condition is

$$\alpha_u q_u^2 + \alpha_d q_d^2 = \frac{\Delta\rho' H}{\rho} \quad (\text{A.8})$$

where  $\Delta\rho' \equiv \rho_s - \rho_{ave} = \Delta\rho(1+Q_d^*)$  and  $Q_d^* = Q_d/Q_0$ .

In application of Eq. (A.8),  $Q_0$ ,  $\Delta\rho$ , and  $H$  are independent variables while  $j$  and  $Q_d$  are dependent variables (unknowns). Because we have one equation describing two unknowns, multiple states are possible (i.e., different combinations of  $j$  and  $Q_d$  for given  $Q_0$ ,  $\Delta\rho$ , and  $H$ ). The data in Figure A.1 clearly indicate this. However, we can solve Eq. A.8 for  $Q_d$  as a function of  $Q_0$ ,  $\Delta\rho$ ,  $H$ , and  $j$ . The result (in terms

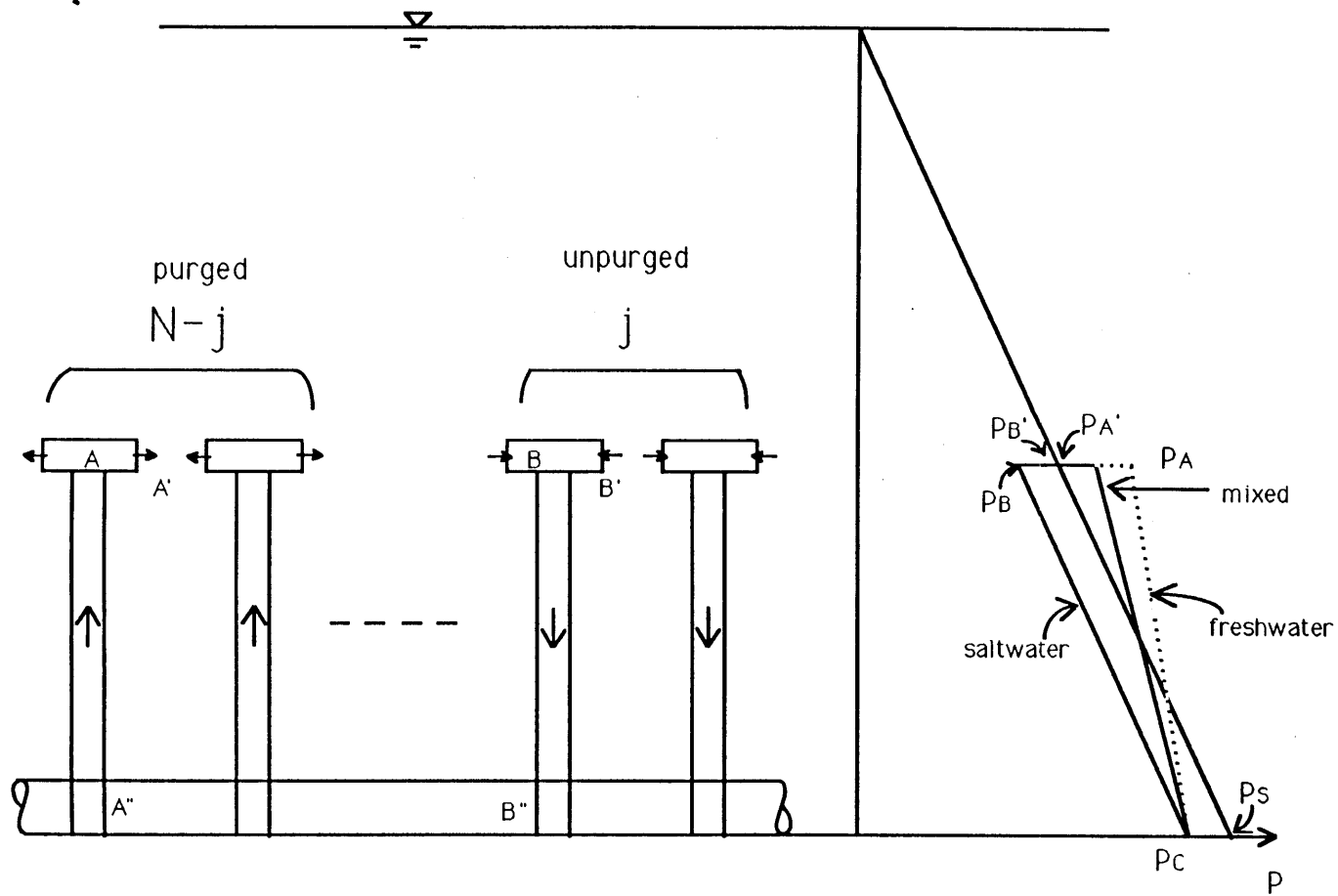


Figure A2 The pressure distribution in purged and unpurged risers with mixed flow

of  $Q_d/Q_M$  vs.  $Q_0/Q_M$ ) is plotted in Figure A.3 using values of  $\Delta\rho$  and  $H$  for the Boston outfall. Note that the value of  $\alpha_u$  was established from the individual riser test depicted in Figure 7 and discussed in Section 4.2. An analogous test was used to determine  $\alpha_d$  which was found to be about 50% greater than  $\alpha_u$ . The maximum value of  $j$  for any  $Q_0/Q_M$  occurs at  $Q_d = 0$  and is the value of  $j_{max}$  given by Eq. (A.1). As  $Q_d$  begins to increase,  $j$  decreases meaning that more downflow is arriving through fewer unpurged risers. For any given  $Q_0$  a maximum  $Q_d$  is possible characterized at  $0 < j < j_{max}$ .

Since there are two dependent variables, Figure A.3 alone can not be used to predict the observed number of unpurged risers, but it can be used to help explain the observations. The observed data of riser purging at various flow rates are plotted in Figure A.1. Most of the points lie above the equivalence line, as was suggested in the discussion above. The following calculations attempt to explain this observation based on the considerations of downflow which lead to Eq. (A.8).

Table A.1 and Figure A.4 compare the downflow rates measured in experiments with those that were calculated at the given condition ( $Q_0$ ,  $\Delta\rho$ ,  $H$ , and observed  $j$ ). Although there is considerable scatter, the data are in general agreement with the theory and much of the scatter can likely be explained by the method in which the observed  $Q_d$  was determined. Observed values were calculated by timing the speed of propagation of dye fronts obtained by introducing red dye into the ocean tank near the discharge ports of several intruding risers. The fronts were timed over a distance of 16 in representing a length-to-diameter ratio of  $16/0.375 = 43$ . Because the intruding flow within the riser was generally laminar, and the time of travel was not large compared with the time scale for crosssectional mixing, the true crosssectional averaged velocity was probably less than the measured front propagation speed. Also the calculated  $Q_d$  was generally based on measurements in

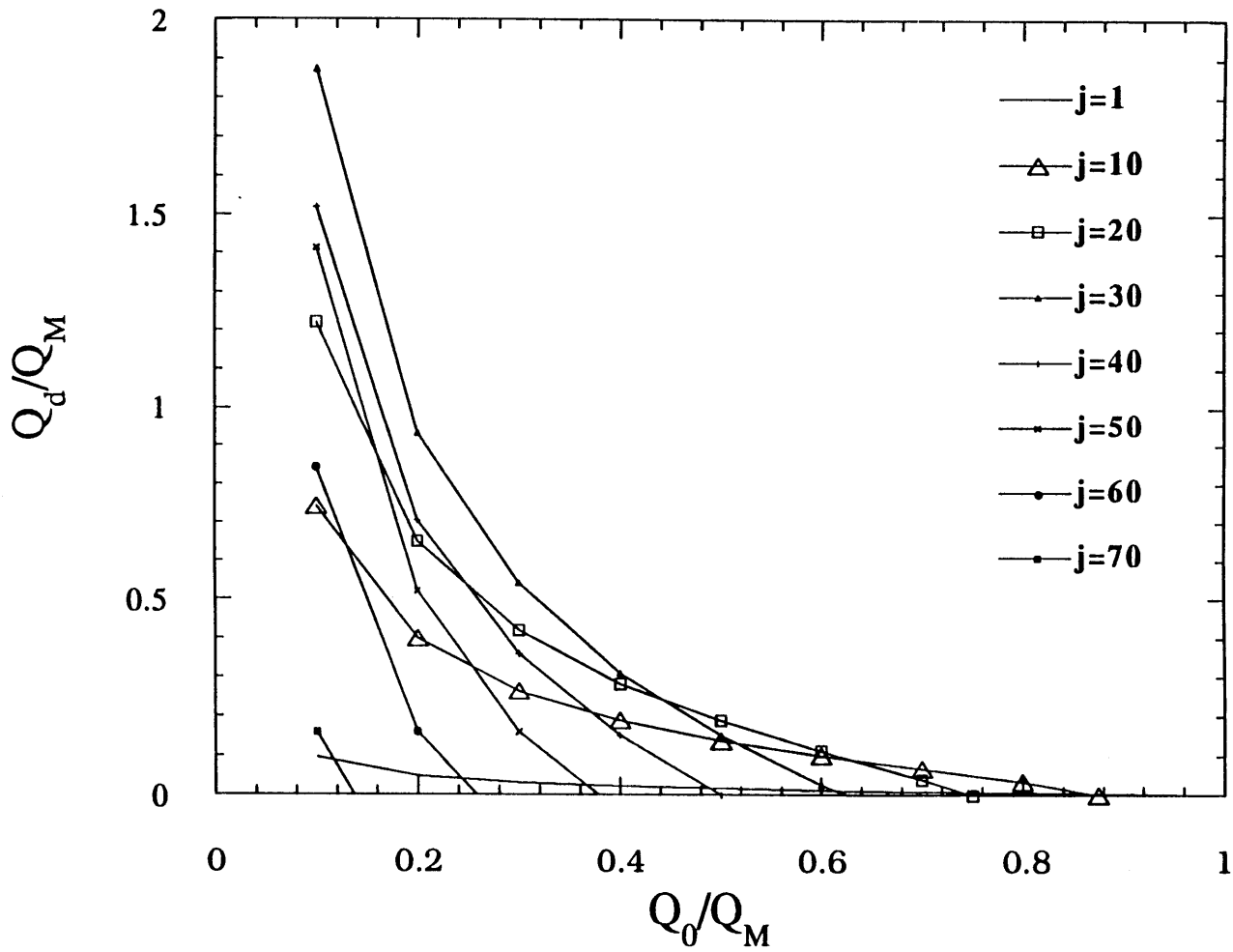


Figure A3 Theoretical total downflow rate vs. effluent flow as a function of number of unpurged risers,  $j$ .  $Q_M$  is the Munro flow.

Table A.1

Comparison of Experimental and Calculated Total Downflow Rates

effluent flow $Q_0$ (gpm)	$Q_0/Q_M$	no. unpurged risers $j$	downflow per riser $q_d$ (in <sup>3</sup> /s)	$Q_d/Q_M$ (data)	$Q_d/Q_M$ (calc)
7.3	0.38	40	0.23	0.13	0.25
10.7	0.55	19	0.59	0.16	0.15
14.3	0.74	7	0.62	0.06	0.04
11.3	0.59	7	1.2	0.13	0.08
8.1	0.42	15	1.2	0.27	0.24
8.2	0.42	32	0.22	0.10	0.25
7.5	0.39	39	0.20	0.11	0.17
6.7	0.35	39	0.29	0.17	0.25
5.8	0.30	41	0.35	0.23	0.38
11.4	0.59	13	0.70	0.16	0.11
15.2	0.79	1	0.95	0.02	0.01
14.3	0.74	1	0.82	0.01	0.01

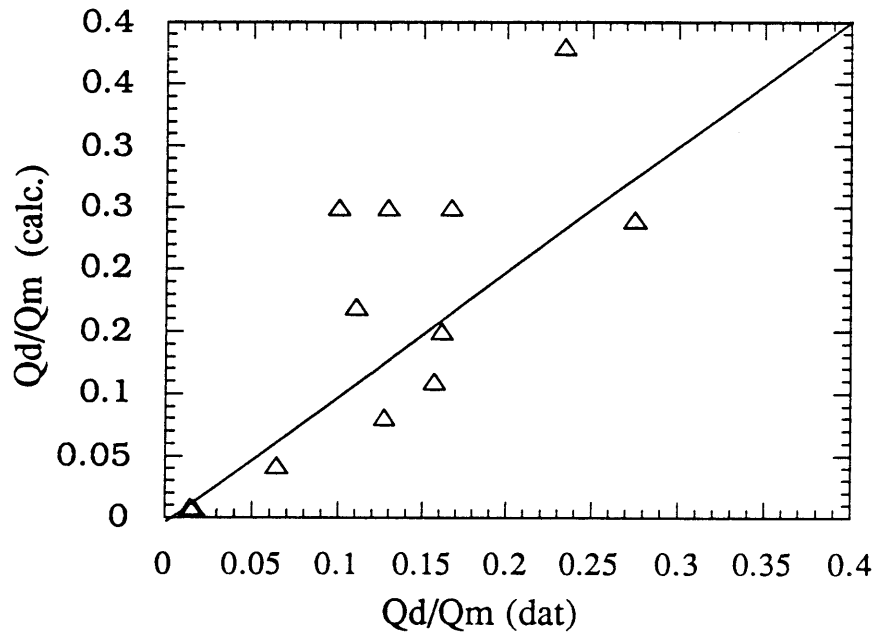


Figure A4 Correlation of calculated downflow with experimental downflow

from three to five risers. Variation in  $q_d$  among risers could have contributed to some of the scatter.

In tests with a transient effluent hydrograph, the observed riser purging data display a hysteresis effect. Figure A.5 shows a typical case in which the purged risers are resistant to unpurging as the tunnel flow is decreased, after an initial increase. This condition is consistent with the fact that multiple states of  $j$  are permissible at any given effluent flow. Although no supporting measurements have been made, this situation presumably persists as long as the decrease in effluent flow is sufficiently slow and the saltwater downflow is sufficiently well-mixed with the effluent flow in the downstream portion of the tunnel. In this way tunnel density changes slowly over time and all purged risers experience the same density. So, even for a large total downflow  $Q_d$  associated with a reduced effluent flow, none of the purged risers would experience a sufficient density increase to collapse and flow down.

One way to determine what value of  $j$  is favorable under equilibrium condition is to perform a stability analysis based on system energy loss. The total rate of energy dissipation in the purged and unpurged risers is

$$E = \alpha_u q_u^3 (N - j) + \alpha_d q_d^3 j \quad (\text{A.9})$$

This varies with the number of unpurged risers  $j$  for any  $Q_0$ . A plot of  $E$  vs.  $j$  for various  $Q_0$ 's is shown in Figure A.6. For all effluent flows the condition of  $j_{\max}$  given by Eq. (A.1) represents a minimum rate of energy dissipation and hence represents a stable equilibrium. The other minimum energy point is with all but one riser purged. This second condition is not expected to occur in practice.



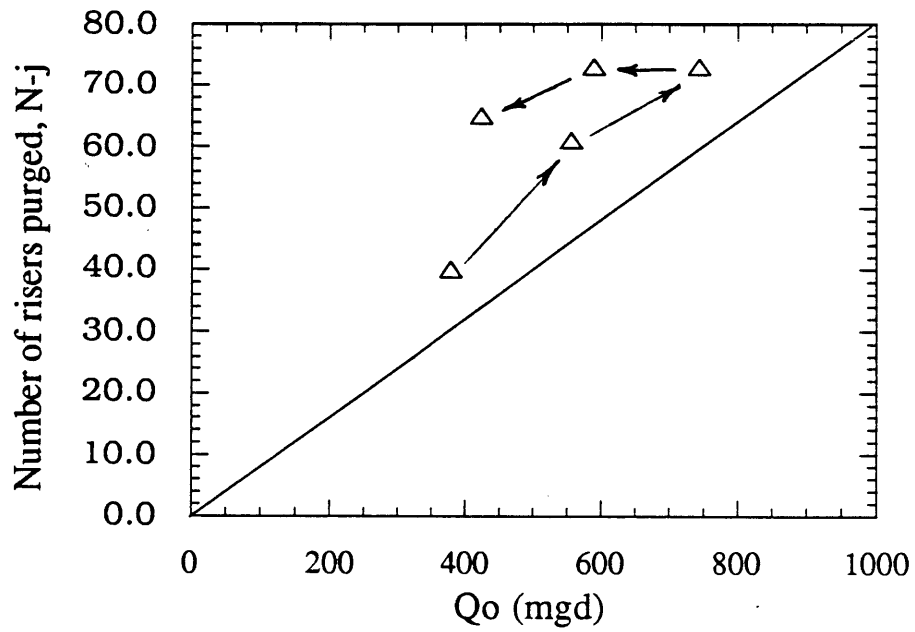


Figure A5 Hysteresis in riser purging with increase and subsequent decrease in tunnel flow

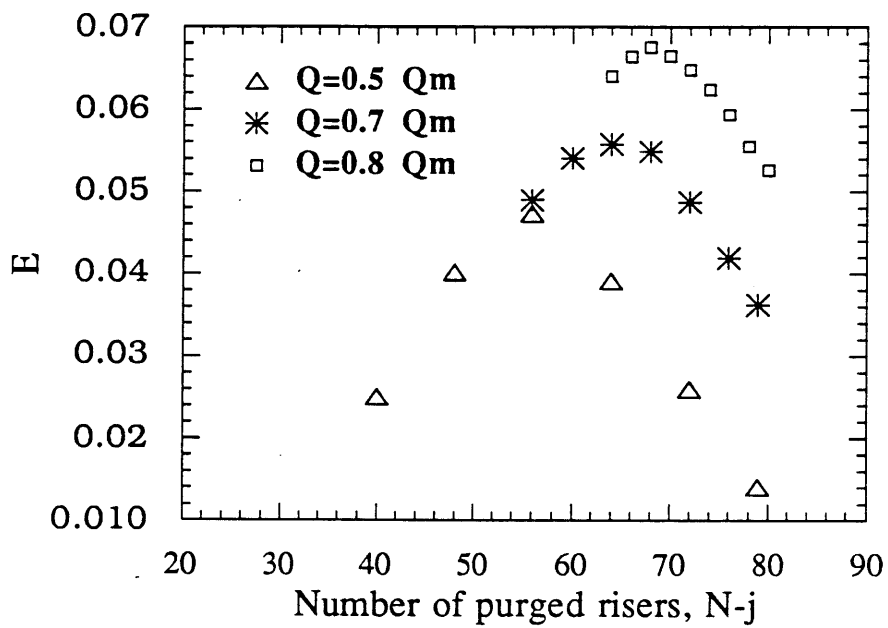


Figure A6 Rate of total energy loss at exit for varying number of purged risers

The results of the stability analysis suggest that the most stable (least energy consuming) state is one with minimum downflow and hence minimum number of purged (maximum number of unpurged) risers. This would argue that, if the flow were allowed sufficient time (beyond the capability of the experimental design), the number of unpurged risers would be more likely to increase, toward the condition of  $j_{\max}$  given by Eq. (A.1), than to decrease.